1671

File Cy.

BRL CR 291

BRL

AD A022478

CONTRACT REPORT NO. 291

ENERGY APPROACHES TO STRUCTURAL VULNERABILITY WITH APPLICATION OF THE NEW BELL STRESS-STRAIN LAWS

Prepared by

J. G. Engineering Research Associates
3831 Menlo Drive
Baltimore, Maryland 21215

March 1976

USA BALLISTIC RESEARCH LABORATORIES
ABERDEEN PROVING GROUND, MARYLAND

UNCLASSIFIED

SECURITY CLASSIFICATION OF THIS PAGE (*When Data Entered*)

REPORT DOCUMENTATION PAGE		READ INSTRUCTIONS BEFORE COMPLETING FORM
1. REPORT NUMBER BRL Contract Report No. 291	2. GOVT ACCESSION NO.	3. RECIPIENT'S CATALOG NUMBER
4. TITLE (*and Subtitle*) Energy Approaches to Structural Vulnerability with Application of the New Bell Stress - Strain Laws		5. TYPE OF REPORT & PERIOD COVERED Contract Report 6. PERFORMING ORG. REPORT NUMBER
7. AUTHOR(*s*) Joshua E. Greenspon		8. CONTRACT OR GRANT NUMBER(*s*) DAAD05-75-C-0731
9. PERFORMING ORGANIZATION NAME AND ADDRESS J G ENGINEERING RESEARCH ASSOCIATES Baltimore, Maryland 21215		10. PROGRAM ELEMENT, PROJECT, TASK AREA & WORK UNIT NUMBERS
11. CONTROLLING OFFICE NAME AND ADDRESS USA Ballistic Research Laboratories Aberdeen Proving Ground, Maryland 21005		12. REPORT DATE MARCH 1976 13. NUMBER OF PAGES 64
14. MONITORING AGENCY NAME & ADDRESS(*if different from Controlling Office*) US Army Materiel Development & Readiness Command 5001 Eisenhower Avenue Alexandria, VA 22333		15. SECURITY CLASS. (*of this report*) UNCLASSIFIED 15a. DECLASSIFICATION/DOWNGRADING SCHEDULE

16. DISTRIBUTION STATEMENT (*of this Report*)

Approved for public release; distribution unlimited.

17. DISTRIBUTION STATEMENT (*of the abstract entered in Block 20, if different from Report*)

18. SUPPLEMENTARY NOTES

19. KEY WORDS (*Continue on reverse side if necessary and identify by block number*)

Energy absorption
Plastic deformation
Isodamage curves
Bell Stress-Strain Laws

20. ABSTRACT (*Continue on reverse side if necessary and identify by block number*)

This report summarizes the various ways in which energy absorbed by a structure can be used in vulnerability studies. Three approaches are explained and mathematical relationships given for each. An extensive presentation is given of a simplified variational approach with applications shown for beams and plates. Finally the new Bell Stress-Strain Laws are applied to compute energy and plastic deformation in beams and plates.

DD FORM 1 JAN 73 1473 EDITION OF 1 NOV 65 IS OBSOLETE

UNCLASSIFIED

SECURITY CLASSIFICATION OF THIS PAGE (*When Data Entered*)

TABLE OF CONTENTS

TABLE OF CONTENTS (cont)

LIST OF ILLUSTRATIONS

I. INTRODUCTION

The complete history of the experimental development of solid mechanics in general and plasticity in particular is traced in the treatise of Professor James F. Bell,[1*] published in 1973. The practical developments in plasticity are rather recent, most of them occurring after 1920. The first complete books on plasticity in English were published by Prager and Hodge[2] and Hill[3] as recently as the early 1950's and to the writer's knowledge, the first and only book devoted completely to dynamic plasticity was published by Cristescu[4] only eight years ago. The field of dynamic plasticity is therefore relatively new compared to dynamic elasticity which is several hundred years old.

The vulnerability of structures depends upon how much deformation they can take and still remain serviceable. Vulnerability implies plastic deformation and failure. Therefore in order to handle the vulnerability problem a knowledge of plastic deformation of structures is a prerequisite. Most of the Army work in vulnerability has of necessity been empirical because the state of the art in plasticity theory has not kept up with the necessities of practical Army problems. The classical theories of plasticity developed over the past twenty or thirty years up to the early 1970's are difficult to apply and leave something to be desired in the way of accuracy in describing material behavior. A summary of the significant vulnerability-oriented calculations for simple structures is contained in a recent paper by Westine and Baker.[5] It is only recently that Bell[6] has developed a new experimentally based general theory that can be applied readily to general large deformation plasticity problems of the type contained in vulnerability studies.

It is the purpose of this report to present the practical vulnerability-oriented approaches using plasticity theory and then introduce some calculations which are based upon Bell's new theory.

*Superscripts refer to references listed at the end of the report.

II. ENERGY THEORIES IN VULNERABILITY

A. Energy approaches in general

The capacity of a structure to absorb energy can be a very useful concept in assessing its vulnerability. Three energy type approaches that have led to fruitful results in vulnerability problems are the variational approach, the asymptotic approximation, and the direct energy equalization. All three use the plastic energy absorbed in the structure under a given configuration called the failure configuration or the mode of failure. This energy absorbed will be denoted by V, where V is a function of the geometry of the structure, its material properties and the deflection component in the direction of the load. These three approaches will be discussed in the order of increasing complication. The objective of all the approaches is to compute the final plastic deflection distribution of the structure as a function of an impulse, load or energy magnitude. Knowing this deflection we can then be in a position to judge whether or not this deformation will constitute a failure.

B. Direct energy equalization[7]

In this approach the energy absorbed by the structure is equated to the energy directed toward the structure either from an explosion or from a series of fragments. The main difficulty with this approach (once V is known for a given failure configuration) is the estimation of the energy given to the target by the explosion or fragments. For blast, in several past reports[8,9] the writer has taken this explosive energy to be the energy flux (energy per unit area) in the explosive wave multiplied by the projected area of the target facing the explosion. For fragments, assuming that perforation takes place, the energy absorbed by the structure is computed by subtracting the residual kinetic energy of the broken up fragments after perforation from the initial kinetic energy of the approaching fragments.

Since this estimation of blast energy does not include any interaction effects between target and blast wave it is therefore bound to be in error. Nevertheless it has led to a basic understanding of the role of energy in predicting the form of the isodamage curves.[7,9] At the present state of the art, we are at the stage where this approach can and should be considerably refined.

C. Asymptotic approximation

The asymptotic energy approach has been formulated by Westine and Baker[5] in a very recent report and can be considered one step more complicated than the direct energy equalization approach discussed above. They equate the energy absorbed in the structure to two separate characteristic energies of the loading in order to narrow down on the damage characteristics. The first of these characteristic energies is the kinetic energy imparted to the structure for short duration impulsive loads. The second characteristic energy is the work performed by the peak load moving through the distance that the structure deforms. Thus two extremes or asymptotes for the energy imparted to the structure are calculated. One of these is in the very short time impulsive loading regime and one is in the long duration quasi static regime. In this way the damage characteristics are approached from both ends of the loading spectrum.

D. The variational approach

In the energy equalization approach no account was taken of the interaction of the blast load with the structure so loading distribution and timewise effects were neglected. In the asymptotic approach some account was taken of the load distribution but timewise effects were only considered in a limiting way. In the variational approach both timewise effects and load distribution characteristics are included. The variational equations for a structure with a given failure configuration were derived in a previous report.[10] For a given failure configuration the system reduces to a single equation for the lateral deflection which is composed of an inertia term depending upon the mass distribution, a stiffness term depending upon the plastic plus elastic energy absorbed in the given configuration and a loading term which is dependent upon the pressure distribution over the structure. The equation, in general, is nonlinear in the deflection, therefore this approach, even though more accurate in principle than the ones described in Sections B and C, can be considerably more complicated if higher order terms in the deflection are involved. There are a number of practical cases, however, which only involve up to quadratic terms in the deflection and these will be discussed later in this report.

III. MATHEMATICAL DETAILS OF THE ENERGY APPROACHES

A. Direct energy equalization

1. General equations

The writer has proposed[7] using the following energy equation for predicting the isodamage characteristics of structures:

$$E_f = \frac{P\,I}{2\,\rho_o\,c_o} + \tfrac{1}{2}\,n\,V^2\,\frac{M}{A} \qquad [1]$$

where E_f = energy density (energy per unit area) which is absorbed by the target structure in undergoing a certain degree of damage

P = side on pressure in the blast impinging on the structure

I = side on impulse in the blast impinging on the structure

ρ_o = mass density of the ambient air

c_o = sound velocity in the ambient air

n = number of fragments hitting the target

V = velocity of the fragments at the target

M = mass of each fragment which hits the target

A = effective area over which the damage takes place

If we multiply equation [1] by A we obtain

$$E_{total} = \frac{P\ I}{2\ \rho_o\ c_o} A + \frac{1}{2}\ n\ V^2\ M \qquad [2]$$

$$E_{total} = E_{blast} + E_{fragments} \qquad [3]$$

The above relations state that the total energy absorbed by the structure undergoing a given level of damage is equal to the blast energy plus the energy imparted by the fragments. The rationale and physical principles behind this relation are discussed thoroughly in the earlier reference.[7] If there are vaporific effects, i.e. if the fragments perforate the structure, hit an internal component or another piece of structure and produce internal pressure because of melting and vaporization, equation [2] still holds because it is tacitly assumed that all energy from the blast or fragments is absorbed by the structure and vaporific effects just represent a conversion of fragment kinetic energy into heat.

2. The experimental approach

Relation [2] can be applied in two ways. The first way is to use an experimental approach. A test must be performed on the structure to obtain one point on the damage curve, i.e. perform either a blast or fragment test to obtain a given level of damage on a structure. If a pure fragment test is performed, then the result can be plotted as a point on the V-M curve as shown in Figure 1.

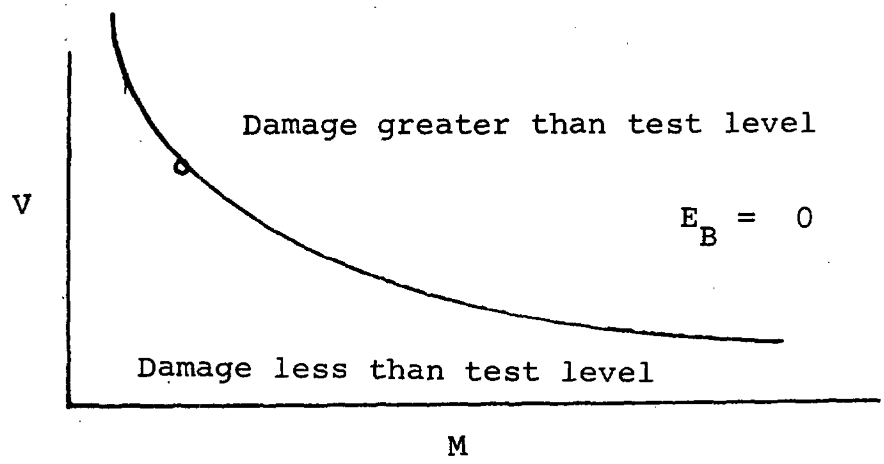

Fig. 1 Fragment Isodamage Curve with No Blast Effects

With n fragments each of mass M hitting the target at velocity V the energy imparted to the target will be

$$E = \tfrac{1}{2}\, nMV^2 \qquad [4]$$

So the isodamage curve is described by the equation

$$V = \sqrt{\frac{E}{\frac{1}{2}\, n\, M}} \qquad [5]$$

This isodamage curve is shown as the curve in Figure 1 drawn through the experimental point. The value of E given by equation[4] is taken as the total energy necessary to do damage of the given level. If blast effects were present then we could describe the blast energy as $PIA/2\rho_o c_o$. Then the fragment energy necessary to afflict the "same damage level"* would be

$$E_f = E - \frac{PI}{2\rho_o C_o} A \qquad [6]$$

The isodamage curve for the fragments would then be described by

$$V = \sqrt{\frac{E_f}{\frac{1}{2}\, n\, M}} \qquad [7]$$

* This has been put in quotes since fragment damage and blast damage do not always afflict the same type of damage.

Similarly if a blast test were run on the structure to do damage at a given level, this point could be plotted on a blast isodamage curve as shown in Figure 2 below.

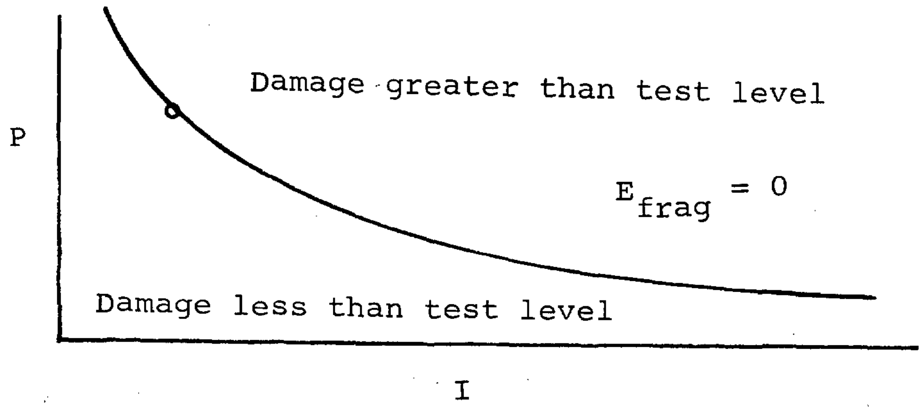

Fig. 2 Blast Isodamage Curve with No Fragment Effects

The energy for doing damage at the given level is given by

$$E = \frac{P\,I}{2\,\rho_o\,c_o} A \qquad [8]$$

So the isodamage curve is given by the relation

$$P = \frac{E}{\dfrac{I}{2\,\rho_o c_o} A} \qquad [9]$$

This curve is shown as the solid line in Figure 2. Now if fragments were present their energy would be described by $\frac{1}{2}nMV^2$ and the blast energy necessary to do the same damage would be

$$E_B = E - \tfrac{1}{2}\,n\,MV^2 \qquad [10]$$

The new isodamage curve for blast would then be given by the relation

$$P = \frac{E_B}{\frac{I}{2\rho_o c_o} A} \qquad [11]$$

3. The theoretical approach

The second way to apply the basic equations is to calculate the total energy under a given failure pattern at a given damage level. Several earlier references[8,9] contain methods for computing blast damage, the most complete presentation being given in Reference 9. Fragment damage and blast damage occurring after fragment damage is discussed in Reference 11. The energy necessary to do fragment damage can be computed from the equation

$$E = \tfrac{1}{2} n M V_{xn}^2 \qquad [12]$$

Eq. [12] is a perforation equation in which n is the number of fragments hitting the target, M is the fragment mass and V_{xn} is the ballistic limit velocity (i.e. the minimum velocity necessary to perforate the target - see Ref. 12). The energy necessary to do a certain blast damage is given in Reference 9 for various patterns of failure. The pattern of failure must be assumed in advance.

4. Checking the theory

The formulas in the previous sections can be validated by using existing data on damage of structures. The way to achieve this is to construct the isodamage curve by using a single data point from an existing test and then checking to see if other points fall along the same curve. To check the theoretical approach of computing the energy absorbed, the energy can be computed by assuming a given pattern of failure, constructing the isodamage curve from this, and then checking experimentally to see if the pressure and impulse or velocity and mass values fall along this curve for equivalent damage.

B. Asymptotic approximation

As an alternative to solving the details of each problem, Westine and Baker[5] have developed a procedure using the absorbed plastic energy to compute the asymptotes for the impulsive and quasi-static regions. They determine these asymptotes by equating the internal plastic work (or strain energy) first to the kinetic energy imparted to the structure to get the asymptote for the impulsive loading regime and then to the work performed by the peak force to get the asymptote for the quasi-static regime. Let V be the plastic energy absorbed (or internal work). This value of V is given for cylindrical shells by eq.[82] and Figs. 22-27 of the writer's 1970 report[9] and for lifting surfaces by eq.[44] - [46] and Table 2 of his 1971 report[11]. Equating this energy absorbed, V, to the kinetic energy imparted to the structure for the impulsive loading regime, the impulse per unit area, I, is given in terms of the energy by the relation[8]

$$I = \sqrt{V \frac{2\mu}{\int_A \bar{f}(A)\,dA}} \qquad [13]$$

where $\bar{f}(A)$ is the impulse distribution on the structure and μ is the mass per unit area of the structure.

In the quasi-static loading regime the work done by the peak load is

$$W = \int_A P(A)\ w(A)\ dA \qquad [14]$$

Equating this to V we obtain for the quasi-static region

$$V = W \qquad [15]$$

(V is a function of the deflection w)

where $P(A)$ is the spatial load distribution and w is the lateral deflection. Some special cases for both axisymmetric and nonaxisymmetric collapse of cylindrical shells were considered by the writer some years ago.[13]

C. Variational approach to the blast problem

1. General equations

There is another approach to the damage problem which looks closer at the individual structure and follows the damage mechanism as it occurs. This approach can best be illustrated by an example. Consider a shell subjected to an enveloping blast. By using variational principles as given in an earlier report[10] the equation for the plastic radial deflection, w, of a cylindrical shell under nonaxisymmetric loading can be written[10]

$$w = w_o(t)\ f_w(A) \qquad [16]$$

where $f_w(A)$ is the spatial distribution of deflection over surface A and $w_o(t)$, the timewise part of the deflection, satifies[10]

$$\ddot{w}_o \int_A \mu\ f_w^2(A)\ dA + \frac{\partial V}{\partial w_o} = \int_A P(A,t)\ f_w(A)\ dA \qquad [17]$$

or written in more familiar single degree of freedom notation

$$m_e \ddot{x} + R_e(x) = P_e(t) \qquad [18]$$

where w_o has been replaced by x and

$$m_e = \int_A \mu\ f_w^2(A)\ dA = \text{the generalized mass}$$

$f_w(A)$ = distribution of deflection w over surface A [19]

$R_e(x) = \dfrac{\partial V}{\partial w_o}$ = the resistance (elastic or plastic)- it can be approximated by a power series in x and

$$P_e(t) = \int_A P(A,t)\ f_w(A)\ dA \qquad [20]$$

where

$$P(A,t) = P_o(A)f(t)$$

$P_o(A)$ = spatial load distribution

$f(t)$ = timewise load distribution [21]

μ = mass per unit area of structure

2. Form of the solution for a long shell (see Ref. 10)

For a perfectly plastic material in which $a/L \ll 1$, $w_o/a \ll 1$ (a = shell radius, L = shell length, w_o = deflection)

$$\frac{\partial V}{\partial w_o} = \sigma_s h L \frac{2}{\sqrt{3}} \int_A f_w(A)\ dA \qquad [22]$$

where h = shell thickness, σ_s = yield stress in pure tension. If we further limit the discussion to exponential timewise loading (i.e. $P(A,t)=\bar{P}(A)\bar{f}(t)=P_o f_p(A) e^{-t/T}$), then the equation of motion [18] takes the same form as eq . [1] of the paper by Westine and Baker,[5] i.e.

$$P e^{-t/T} - f = m\ddot{x} \qquad [23]$$

where

$$P = \int_A P_o(A)\ f_w(A)\ dA = \int_A P_o\ f_p(A)\ f_w(A)\ dA \qquad [24]$$

$f_p(A)$=spatial load distribution

$$f = \sigma_s h\ l \frac{2}{\sqrt{3}} \int_A f_w(A)\ dA \qquad m = \int_A \mu\ f_w^2(A)\ dA$$

The solution curve is exactly the one shown by Westine and Baker[5] as Figure 2 of their paper with the above parameters which depend upon the deformed shape, $f_w(A)$, the spatial load distribution, $f_p(A)$ and the other physical characteristics of the shell. This curve is shown in Fig. 3

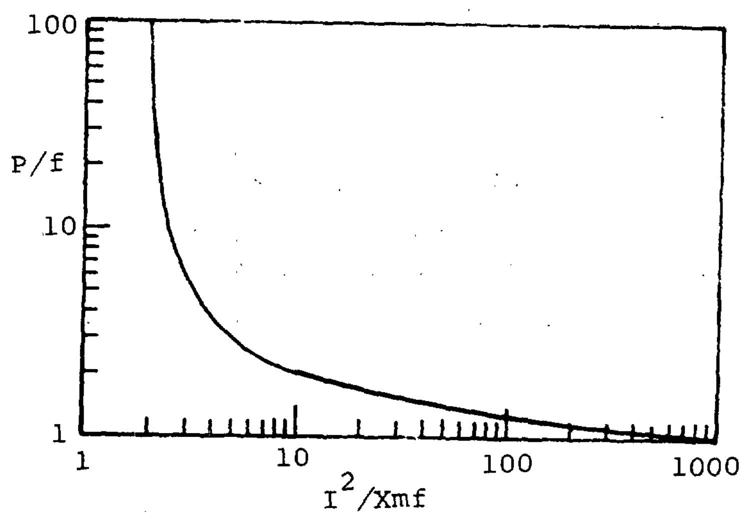

Fig. 3 P - I Diagram for Rigid - Plastic Model[5]

In this curve

$$I = \int_0^{\infty} P\, e^{-t/T}\, dt = \int_0^{\infty} P_o\, e^{-t/T}\, dt \int_A f_p(A)\, f_w(A)\, dA$$

X = maximum deflection (i.e. (w_o)max.)

3. Interpretation in terms of conventional P-I isodamage curves

An interpretation of this scaled P-I curve as it relates to damage problems is certainly in order here. This curve (fig. 3) really gives the solution to the plastic problem in nondimensional form. For a given set of values of P, f, I, m we can obtain the value of I^2/Xmf resulting from a certain value of P/f and then calculate the value of the maximum deflection, X, from this result. The conventional isodamage curve is a plot of pressure vs. impulse as shown in Figure 4.

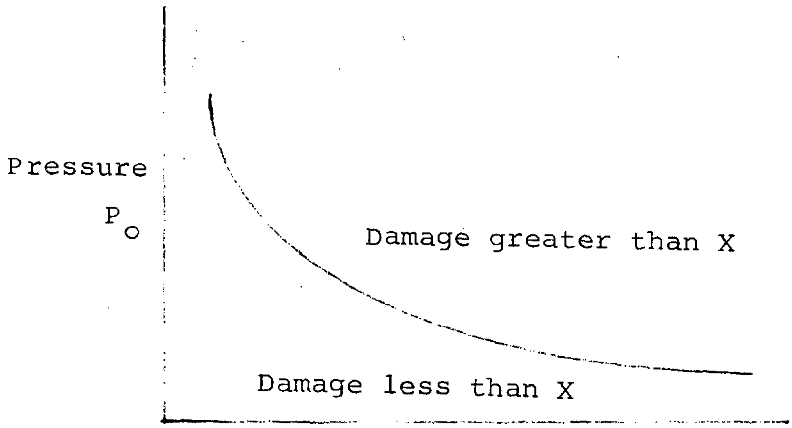

$$\text{Impulse } I_o = \int_0^{\infty} P_o\, e^{-t/T}\, dt = P\,T$$

Fig. 4 Conventional Isodamage Curve

The conventional curve of Figure 4 is obtained from the nondimensional solution curve of Figure 3 as follows:

a. Choose values of P/f from Fig. 3 and calculate P_o from the relations

$$P = f\,(P/f) \quad \text{and} \quad P_o = \frac{P}{\int_A f_p(A)\; f_w(A)\; dA} \qquad [26]$$

b. Pick off values of I^2/Xmf from Fig. 3 corresponding to the particular values of P/f selected in "a" above. Compute I from the relation

$$\frac{I^2}{X\,m\,f} = \text{Value obtained from curve} = \bar{I} \qquad [27]$$

Assume **X** for a given damage level, thus $I^2 = \bar{I}\;X\,m\,f$

$$I_o^2 \left[\int_A f_p(A)\; f_w(A)\; dA \right]^2 = \bar{I}\;X\,m\,f$$

$$\textbf{therefore} \qquad I_o = \frac{\sqrt{\bar{I}\;X\,m\,f}}{\int_A f_p(A)\; f_w(A)\; dA} \qquad [28]$$

Note that the conventional isodamage curve calculated in this way (as contrasted with that shown in Section IIIA) will not have zero asymptotes, i.e. it will give infinite pressure for some finite value of impulse instead of infinite pressure for zero impulse. Likewise it will give infinite impulse for some finite value of pressure instead of infinite impulse for zero pressure. This is therefore a more accurate way to obtain the isodamage curve for blast on a given structure if the load distribution is known.

IV. VARIATIONAL SOLUTIONS FOR BEAMS AND PLATES

A. General background

The general form of the variational equation is given by equation [18]. If the resistance function, R_e is a constant then the equation takes the same form as the simple Westine-Baker[5] equation (i.e. eq. [23]). For these cases the curve of Westine and Baker (i.e. Fig. 3) can be used as a nondimensional isodamage curve as long as the proper interpretation is given to each of the terms.

B. Plastic deformation of cantilever beams

Westine and Baker[5] have computed the plastic strain energy of a cantilever beam. This energy, V, is

$$V = \frac{\pi\,\sigma_y\; b\; h^2\; w_o}{16\;L} \qquad [29]$$

where σ_y = yield stress

b = width of beam

h = thickness of beam

L = length of beam

w_o = maximum tip deflection

Using a deflection shape of $w = w_o \left(1 - \cos \frac{\pi x}{2L}\right)$ [30]

The resistance function, R_e for this case turns out to be

$$R_e = \frac{\partial V}{\partial w_o} = f = \frac{\pi \sigma_y b h^2}{16 L} \quad [31]$$

The generalized mass, m_e is

$$m_e = \int_A \mu f_w^2(A)\, dA = b \int_0^L \rho h \left(1 - \cos \frac{\pi x}{2L}\right)^2 dx = .23\, b\, h\, L \quad [32]$$

For a uniformly distributed load the generalized loading function is

$$P = P_o \int_A f_p(A)\, f_w(A)\, dA \qquad f_p(A) = 1 \quad [33]$$

$$P = P_o (.36\, b\, L)$$

Thus

$$P/f = \frac{P_o (.36\, b\, L)\, 16\, L}{\pi \sigma_y b h^2} = \frac{P_o}{\sigma_y} \frac{16 L^2 (.36)}{\pi h^2} = \frac{P_o}{\sigma_y} \frac{L^2}{h^2} (1.83) \quad [34]$$

and

$$\frac{I^2}{X\, m\, f} = \frac{I_o^2 (.36\, b\, L)^2}{X (.23\, b \rho h L) \left(\frac{\pi \sigma_y b h^2}{16 L}\right)} = \frac{I_o^2}{\rho h w_o \sigma_y} \frac{L^2}{h^2} (2.88) \quad [35]$$

So the curve of P/f vs. I^2/Xmf converts for a cantilever to a curve of

$$1.83 \frac{P_o}{\sigma_y} \frac{L^2}{h^2} \quad \text{vs} \quad 2.88 \frac{I_o^2}{\rho h w_o \sigma_y} \frac{L^2}{h^2}$$

Cantilevers made from 6061-T6 aluminum which were 12 inches long and .051 inches thick were tested at BRL.[14] For this material σ_y = 40,000 psi, ρ = .000255 lb. sec.^{2}/in.^{4}. The asymptotes of the isodamage curve are calculated directly as follows:

For the impulsive loading regime $I^2 / X\, m\, f = 2.0$

so

$$2.88 \frac{I_o^2}{\rho\, h\, w_o\, \sigma_y} \frac{L^2}{h^2} = 2.0 \qquad [36]$$

therefore

$$\frac{w_o}{L} = 1.44 \frac{L}{h} \left(\frac{I_o}{h\sqrt{\rho\,\sigma_y}} \right)^2$$

For the quasi-static loading regime $P_o / f = 1$

$$[37]$$

so

$$1.83 \frac{P_o}{\sigma_y} \frac{L^2}{h^2} = 1 \qquad \text{or} \qquad \frac{P_o}{\sigma_y} = .54 \frac{h^2}{L^2}$$

The value for the quasi-static regime checks with the Westine-Baker value[5] since they take account of the deflection distribution in their calculation of the quasi-static asymptote. The value calculated for the impulsive regime does not check since they omitted the effect of deflection distribution on the Kinetic energy. If the energy principle is derived from the variational equation, it is found that[15]

$$\int_0^{x_m} P_e(t)\, dx = \int_0^{x_m} R_e(x)\, dx \qquad [38]$$

where

$$P_e(t) = \int_A P(A,t)\, f_w(A)\, dA \qquad R_e(x) = \frac{\partial V}{\partial x} \qquad [39]$$

Under these circumstances the result for the impulsive loading region is[15]

$$W_{P_e} = \frac{H_{me}^2}{2\, m_e} \qquad [40]$$

where W_{P_e} = strain energy absorbed by the structure (internal work done by the structure)

$$H_{me} = \int_0^T P_e(t)\, dt \quad (\textbf{the generalized impulse})$$

$$m_e = \int_A \mu\, f_w^2(A)\, dA \quad (\textbf{the generalized mass}) \qquad [41]$$

Under these circumstances $\dfrac{\pi \sigma_y b h^2 w_o}{16 L} = .56 \dfrac{I_o^2 b L}{2 \rho h}$ [42]

so $$\frac{w_o}{L} = 1.42 \left(\frac{I_o}{h\sqrt{\rho \sigma_y}} \right)^2 \frac{L}{h}$$

As is shown in Figure 5 this correction gives results which fit the data somewhat better than the Westine-Baker curve at lower permanent sets.

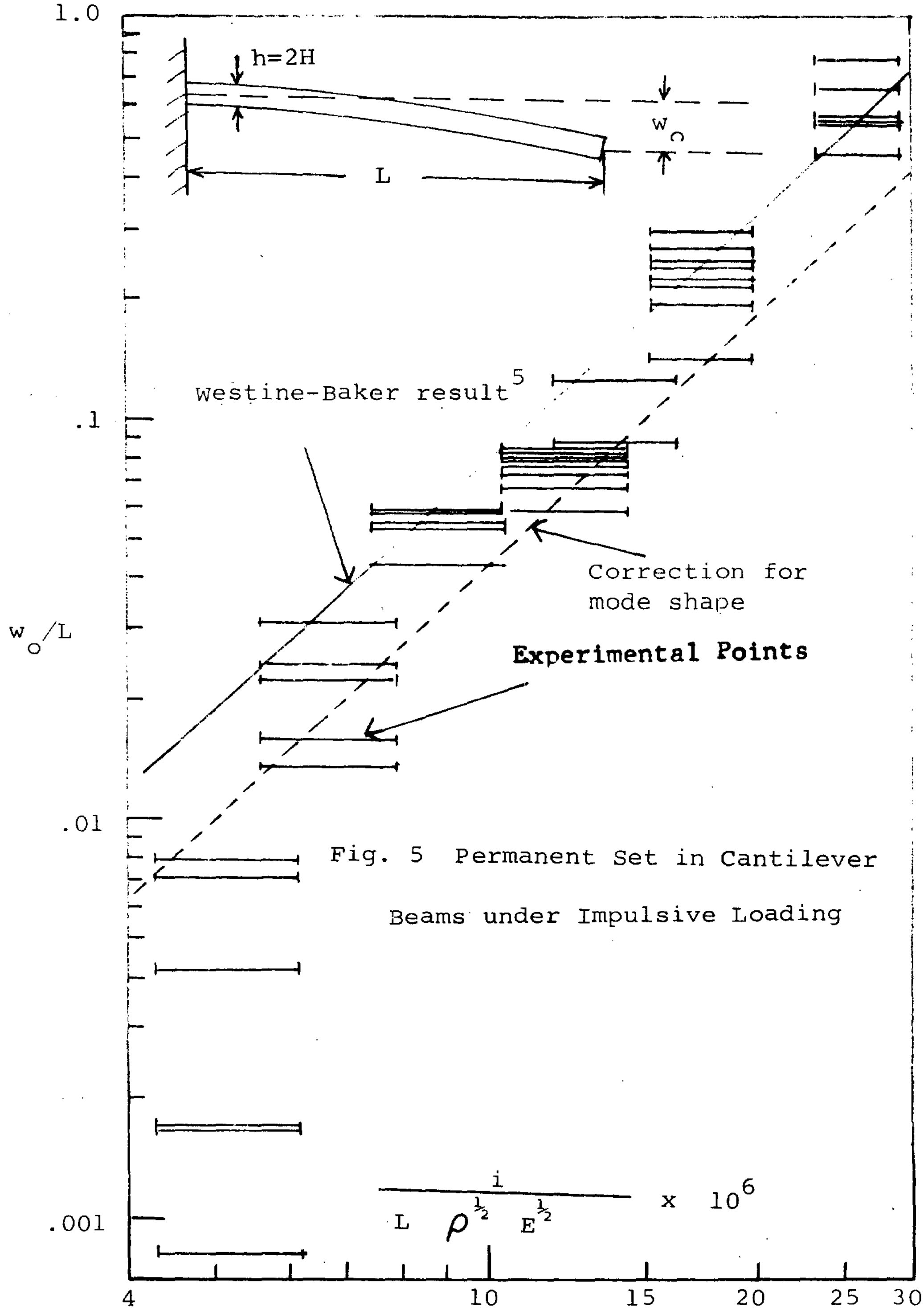

Fig. 5 Permanent Set in Cantilever Beams under Impulsive Loading

The nondimensional isodamage curve for the cantilever is then found by replacing the ordinate and abscissa of Figure 3 by

$$1.83 \quad \frac{P_o}{\sigma_Y} \frac{L^2}{h^2} \qquad \text{and} \qquad 2.88 \frac{I_o^2}{\rho \, h \, w_o \, \sigma_Y} \frac{L^2}{h^2} \qquad \text{respectively}$$

The conventional isodamage curve for this cantilever is shown in Fig. 6.

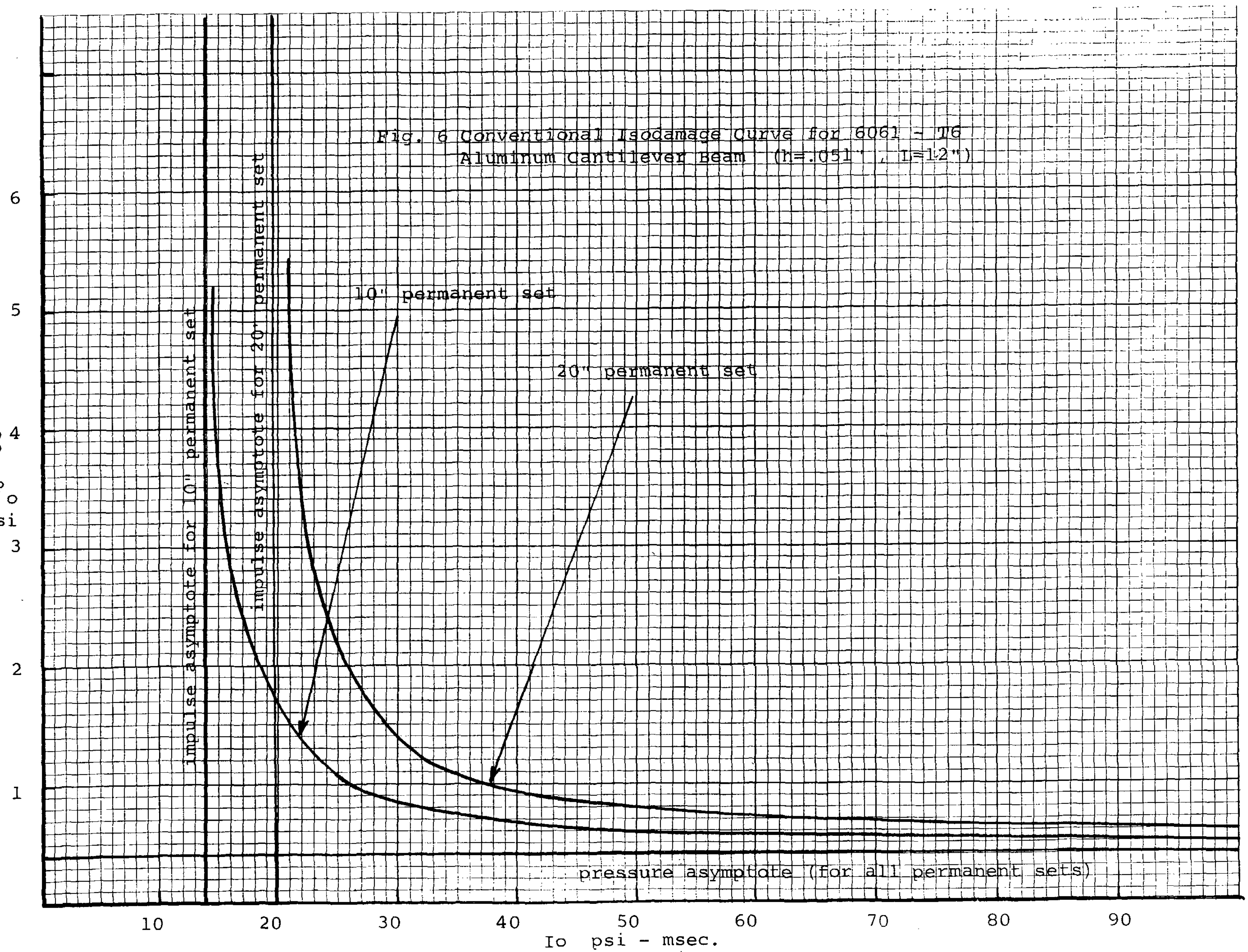

Fig. 6 Conventional Isodamage Curve for 6061 - T6 Aluminum Cantilever Beam (h=.051", l=12")

There are several basic principles which can be learned from this example. Firstly, the isodamage asymptote for pressure is a constant for the perfectly plastic beam, i.e. it is independent of the level of damage. Secondly, the asymptote for impulse is dependent upon the damage. The pressure asymptote really defines a collapse pressure for the beam under static loading.

C. Plastic deformation of uniform simply supported beams

For the case of a perfectly plastic simply supported beam of rectangular section the strain energy is given by[5]

$$V = \frac{8\, M_y\, w_o}{L} \qquad [43]$$

where $M_y = \frac{\sigma_y\, b\, h^2}{4}$ yield moment

b = width of beam

h = thickness of beam [44]

L = length of beam

Thus

$$f = R_e = \frac{\partial V}{\partial w_o} = \frac{8\, M_y}{L} \qquad [45]$$

The generalized mass is (using a deflection shape of $w = w_o \sin \frac{\pi x}{L}$)

$$m_e = \int_A \mu\, f_w^2(A)\, dA = b \int_0^L \rho\, h \sin^2 \frac{\pi x}{L}\, dx = .5\, \rho\, h\, b\, L \qquad [46]$$

For a uniformly distributed load the generalized force is

$$P = P_o \int_A f_p(A)\, f_w(A)\, dA \qquad f_p(A) = 1 \qquad [47]$$

So $P = .64\, b\, L\, P_o$

So for this case

$$P/f = \frac{P_o\,(.64\, b\, L)}{\frac{8}{L}\,\frac{\sigma_y\, b\, h^2}{4}} = \frac{P_o}{\sigma_y}\,\frac{L^2}{h^2}\,(.32) \qquad [48]$$

$$I^2/\, X\, m\, f = \frac{I_o^2\,(.64\, b\, L)^2}{w_o\,(.5\, b\, L\, \rho\, h)\left(\frac{8\, \sigma_y\, b\, h^2}{4\, L}\right)} = \frac{I_o^2}{\rho\, h\, w_o\, \sigma_y}\,\frac{L^2}{h^2}\,(.64)^2$$

So the curve of P/f vs $I^2/\, X\, m\, f$ converts for a simply supported beam to a curve of $.32\, \frac{P_o}{\sigma_y}\,\frac{L^2}{h^2}$ vs $.41\, \frac{I_o^2}{\rho\, h\, w_o\, \sigma_y}\,\frac{L^2}{h^2}$

The asymptote for the impulsive loading region is

$$.41 \frac{I_o^2}{\rho h w_o \sigma_y} \frac{L^2}{h^2} = 2 \quad \text{So} \quad \frac{w_o}{L} = .2 \left(\frac{I_o^2}{h\sqrt{\rho \sigma_y}} \right)^2 \frac{L}{h} \quad [49]$$

In the paper by Westine and Baker[5] their $2\ell = L$ so that the above value comes very close to their value. The slight difference is probably due to the fact that the shape was considered here in computing the kinetic energy. The asymptote for the quasi-static regime is given by

$$.32 \frac{P_o}{\sigma_y} \frac{L^2}{h^2} = 1 \quad \text{or} \quad \frac{P_o}{\sigma_y} = 3\,(h/L)^2 \quad [50]$$

which is exactly the value given by Westine and Baker.[5]

D. Plastic deformation of uniform simply supported plates

For the case of simply supported plates Westine and Baker[5] find that the strain energy is given by (assuming a perfectly plastic material and plate dimensions of a, b, h - width, length, thickness respectively).

$$V = \sigma_y h^2 w_o \left(\frac{b}{a} + \frac{a}{b} \right) + \frac{4}{\sqrt{3}} \sigma_y h^2 w_o + \frac{\pi^2}{8} \sigma_y h w_o^2 \left(\frac{b}{a} + \frac{a}{b} \right) + \frac{4}{\sqrt{3}} \sigma_y h w_o^2 \quad [51]$$

The terms linear in w_o represent bending terms and those quadratic in w_o arise from tension in the middle surface of the plate.

Let w be given by $$w = w_o \sin \frac{\pi x}{a} \sin \frac{\pi y}{b} \quad [52]$$

The terms in the variational equation are then

$$m = m_e = \int_0^a \int_0^b \rho h \sin^2 \frac{\pi x}{a} \sin^2 \frac{\pi y}{b}\, dx\, dy = \frac{\rho h a b}{4} \quad [53]$$

$$P = P_e = P_o \int_0^a \int_0^b \sin \frac{x}{a} \sin \frac{y}{b}\, dx\, dy = P_o\, 4 \frac{a b}{\pi^2}$$

The variational equation becomes

$$m_e \ddot{w}_o + \frac{\partial V}{\partial w_o} = P_e \bar{f}(t) \quad \text{so} \quad [54]$$

$$m \ddot{w}_o + f_1 w_o + f = P \bar{f}(t)$$

Again using the typical exponentially decaying pulse

$$\bar{f}(t) = e^{-t/T} \quad [55]$$

We obtain $$m \ddot{w}_o + f_1 w_o = P e^{-t/T} - f \quad [56]$$

$$f_1 = \frac{\pi^2}{4} \sigma_y h \left(\frac{b}{a} + \frac{a}{b} \right) + \frac{8}{\sqrt{3}} \sigma_y h$$

where

$$f = \sigma_y h^2 \left(\frac{b}{a} + \frac{a}{b} \right) + \frac{4}{\sqrt{3}} \sigma_y h^2 \qquad [57]$$

This is a linear differential equation, the solution of which is as follows:

The initial conditions are $w_o(0) = \dot{w}_o(0) = 0$

Thus

$$p_1 = \sqrt{f_1/m} \qquad [58]$$

$$w_o(t) = \frac{1}{m\, p_1} \int_0^t P\, e^{-\mathcal{T}/T} \sin p_1 (t - \mathcal{T})\, d\mathcal{T} - \frac{f}{m\, p_1} \int_0^t \sin p_1 (t - \mathcal{T})\, d\mathcal{T} \qquad [59]$$

Integrating, we obtain

$$w_o(t) = \frac{P\,T}{m\, p_1} \left[\frac{\sin p_1 t - p_1 T \cos p_1 t + p_1 T\, e^{-t/T}}{1 + (p_1 T)^2} \right] - \frac{f_1}{m\, p_1^2} \left(1 - \cos p_1 t \right) \qquad [60]$$

The maximum deflection, X is determined from the criterion that $\dot{w}_o = 0$ when $w_o = (w_o)_{max}$ $(= X)$

i.e. when

$$\frac{P}{f}\, p_1 T \left[\frac{\cos p_1 t + p_1 T \sin p_1 t - e^{-t/T}}{1 + (p_1 T)^2} \right] - \sin p_1 t = 0 \qquad [61]$$

The lowest value of t/T which satisfies this equation gives the time at which the maximum deflection will occur. If we let $\alpha = p_1 T$ then the above equation becomes

$$\frac{P}{f}\, \alpha \left[\frac{\cos \alpha\, t/T + \alpha \sin \alpha\, t/T - e^{-t/T}}{1 + \alpha^2} \right] - \sin \alpha\, t/T = 0 \qquad [62]$$

where

$$\alpha = p_1 T = T \sqrt{f_1/m} \qquad [63]$$

The minimum values of t/T which satisfy this equation are plotted as a function of P/f for various α in Figs. 7,8. The deflection can then be written as

$$\frac{X\, m\, \alpha}{P\, T^2} = \left[\frac{\sin \alpha\, t/T - \alpha \cos \alpha\, t/T + \alpha\, e^{-t/T}}{1 + \alpha^2} \right] - \frac{1}{\frac{P}{f}\, \alpha} \left(1 - \cos \alpha\, t/T \right) \qquad [64]$$

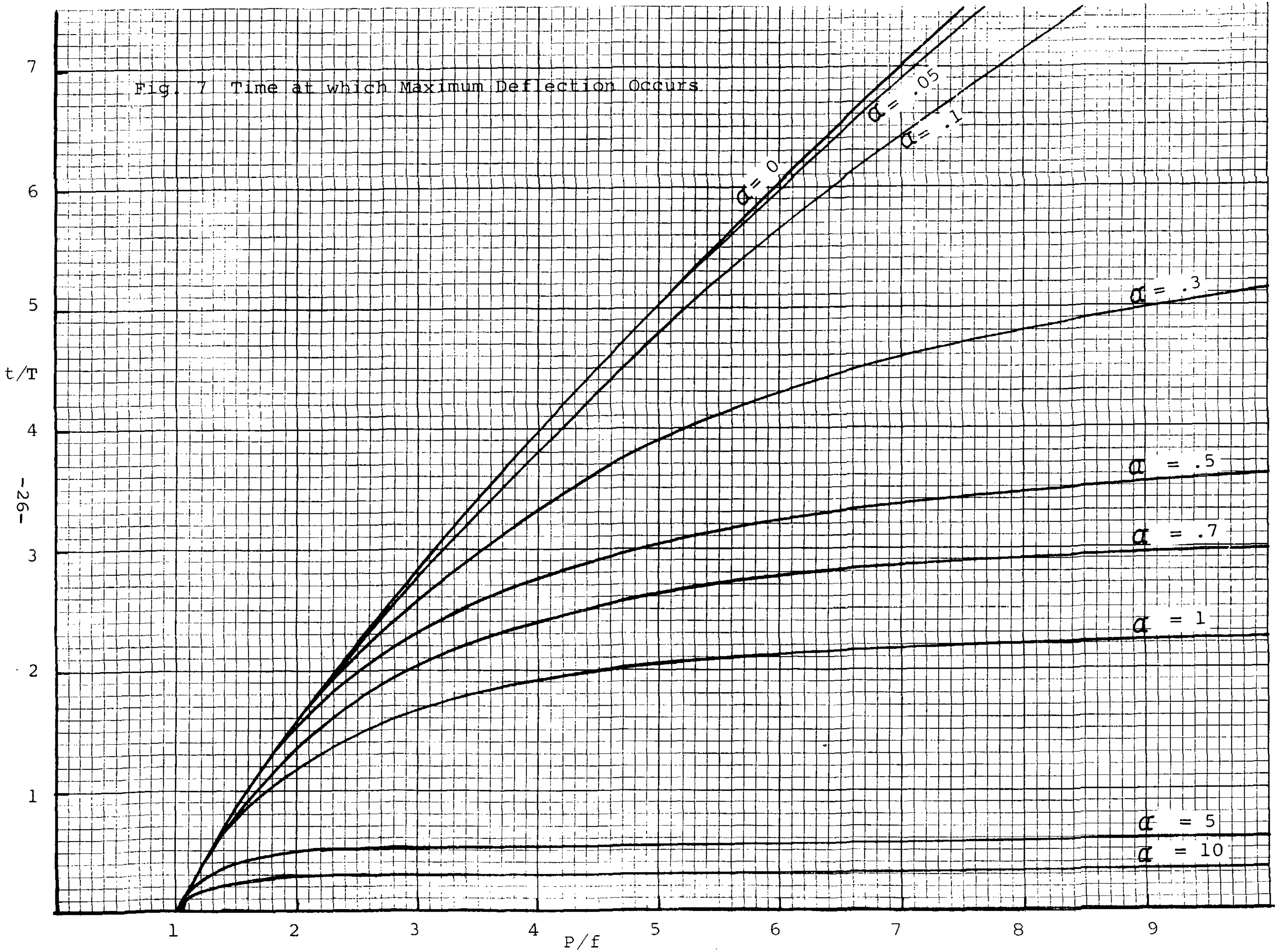

Fig. 7 Time at which Maximum Deflection Occurs

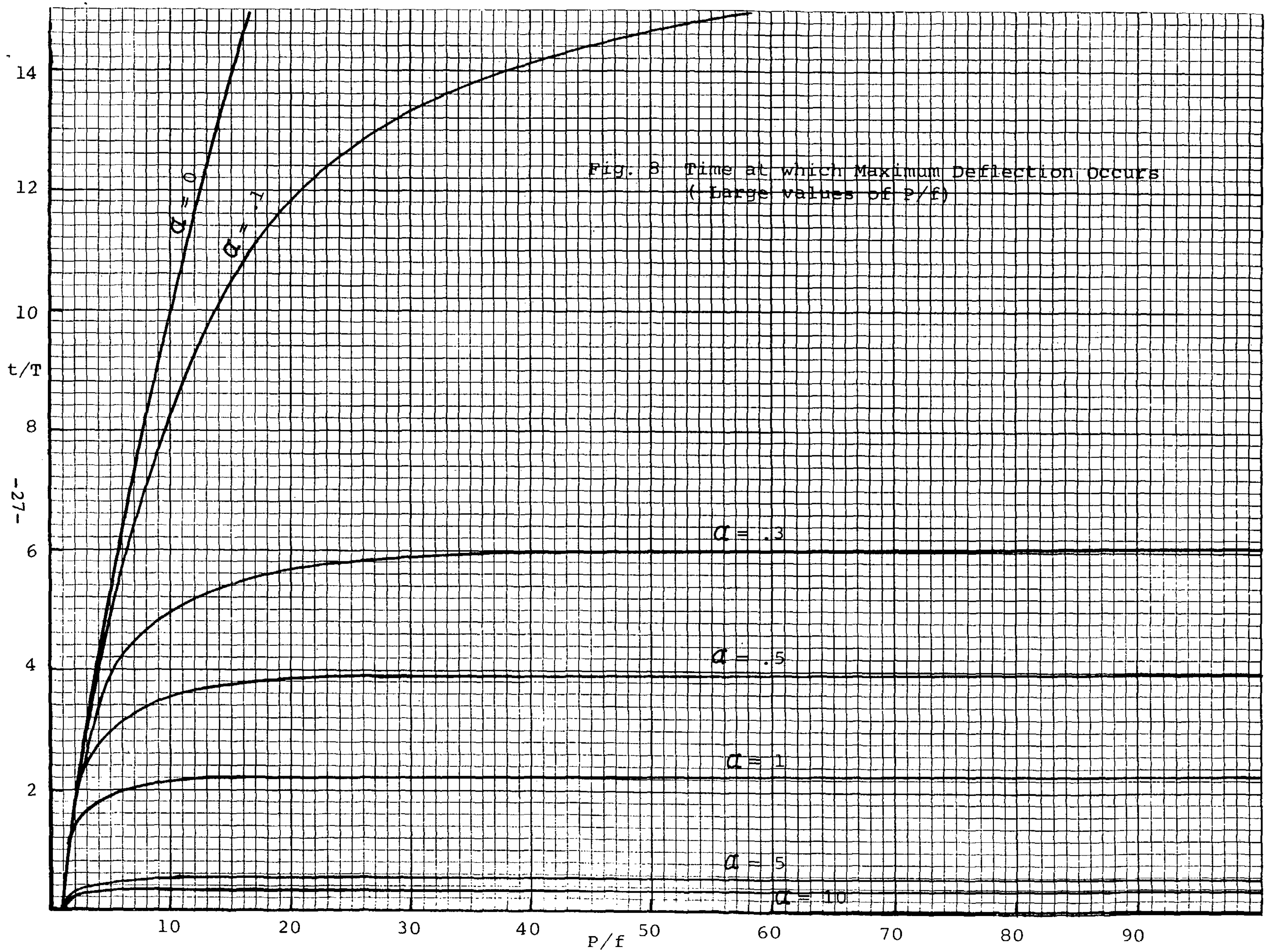

Fig. 8 Time at which Maximum Deflection Occurs
(Large values of P/f)

In order to compare the results with the Westine-Baker results (for $\alpha = 0$) we plot P/f as ordinate and I^2/Xmf as abscissa. The resulting curves are shown in Figure 9a for various values of α. Note that for $\alpha > 0$ there is no vertical asymptote as found by Westine and Baker[5] for $\alpha = 0$. The horizontal asymptote for nondimensional pressure remains the same for all α. Figure 9b contains the same solution curves plotted with a different abcissa. This figure illustrates how increasing α increases the stiffness of the plate. The parameter α is a measure of the tension in the middle surface of the plate. The solution curves are general and can be applied to any system in which the energy can be expressed as a quadratic function of the deflection.

V. APPLICATIONS USING THE BELL STRESS-STRAIN LAWS

A. General background

For about a decade Professor James F. Bell of the Johns Hopkins University has been developing techniques and producing extensive experimental stress-strain data on many materials under uniaxial loading for both the static case and the dynamic case involving high rates of strain. Recently he has also made extensive studies on biaxial loading in the static regime. Most of Bell's work which is applicable here is contained in two recent references.[1,6] He has developed both deformation and flow laws for alloys under uniaxial, shear, and biaxial loading. In the present report the writer will illustrate the application of Bell's Laws to both one and two dimensional cases of structures under impulse loading.

The one dimensional tension-compression stress-strain law given by Bell[6] for plastic deformation is

$$\begin{aligned} \sigma &= E\epsilon && \text{if} \quad \epsilon < \epsilon_y \\ \sigma &= \sigma_y + c\sqrt{\epsilon - \epsilon_y} && \text{if} \quad \epsilon_y \leqslant \epsilon \leqslant \epsilon_c \\ \sigma &= c\sqrt{\epsilon - \epsilon_c + \frac{\epsilon_N}{\lambda_N}} && \text{if} \quad \epsilon > \epsilon_c \end{aligned} \qquad [65]$$

In the above equations

σ = tensile or compressive stress

ϵ = tensile or compressive strain

E = elastic modulus

σ_y = yield stress

ϵ_y = yield strain

ϵ_c = critical strain (given by Bell[6])

$c = \lambda_N^{3/2}\, \bar{m}^{3/2}\, \beta_s$ given by Bell[6])

ϵ_N, λ_N = parameters given by Bell[6]

Fig. 9 Nondimensional Solution Curves for Plates under Large Plastic Deformation

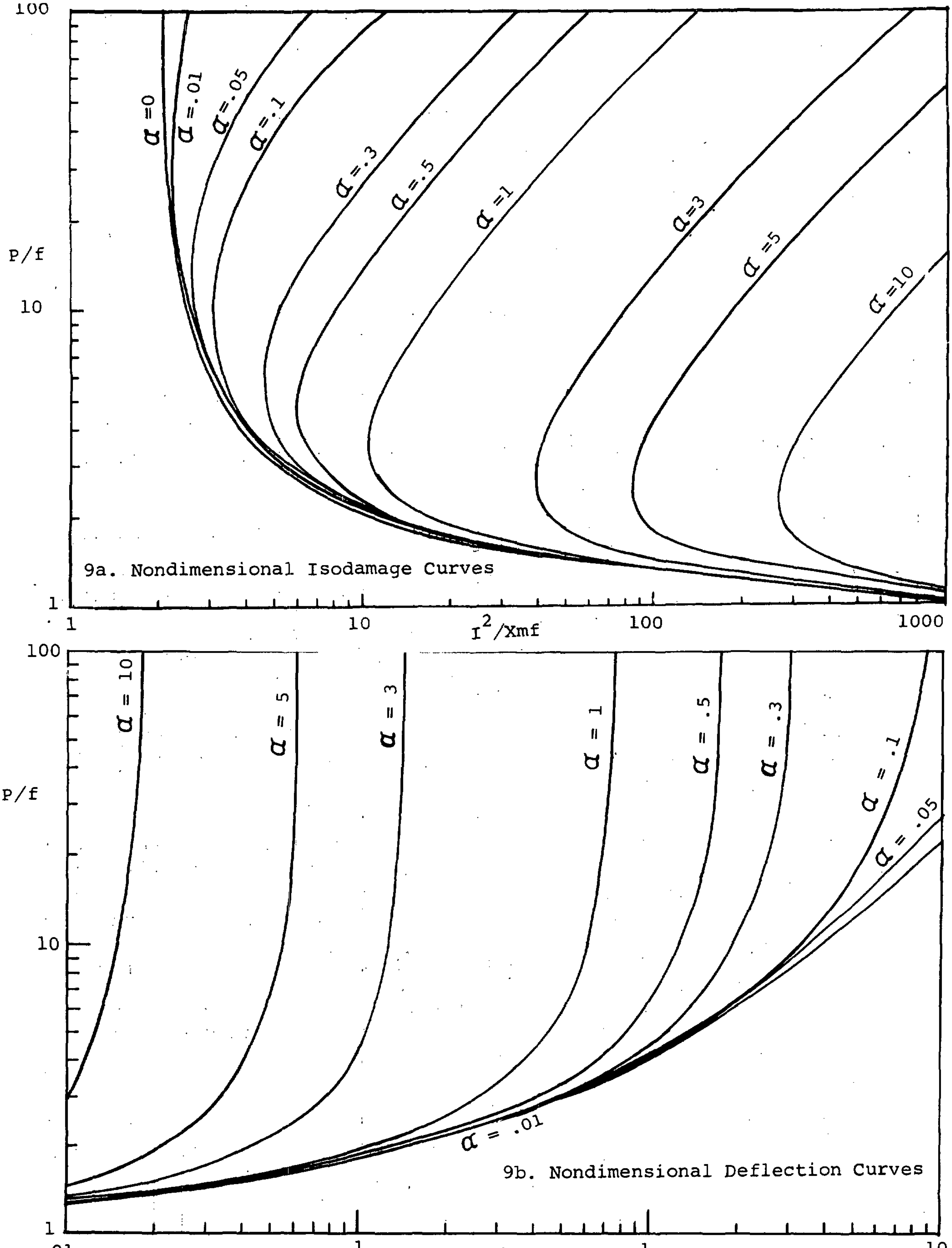

Each of the parameters given by Bell[6] is associated with a particular physical phenomena of the material as explained in Bell's previous work.[1] There is an analogous one dimensional shear law which follows the same form as the one dimensional tension-compression relation.

For biaxial stress Bell[6] gives as the deformation law

$$\begin{aligned} T &= E\,\Gamma && \text{if} \quad \Gamma < \Gamma_Y \\ T &= T_Y + \bar{c}\sqrt{\Gamma - \Gamma_Y} && \text{if} \quad \Gamma_Y \leq \Gamma \leq \Gamma_c \\ T &= \bar{c}\sqrt{\Gamma - \Gamma_c + \frac{\Gamma_N}{\lambda_N}} && \text{if} \quad \Gamma > \Gamma_c \end{aligned} \qquad [66]$$

$$\text{where} \quad \bar{c} = \lambda_N^{3/2}\ \bar{K}^{3/2}\ \beta_s$$

where

$$T = \sqrt{\tfrac{2}{3}}\sqrt{\sigma_X^2 + \sigma_Y^2 - \sigma_X\sigma_Y + 3\tau_{XY}^2} \quad = \text{octahedral shear stress} \qquad [67]$$

$$\Gamma = \sqrt{2}\sqrt{\epsilon_X^2 + \epsilon_Y^2 + \epsilon_X\epsilon_Y + \frac{\gamma_{XY}^2}{4}} \quad = \text{octahedral shear strain}$$

All the parameters involved in the above equations are given by Bell[6] and explained thoroughly in his treatise[1] and his many earlier papers.

B. Application to one dimensional problems-bending of beams

1. Moment curvature relationship

In the classical theory of elasticity the bending moment, M, in a beam is given in terms of the curvature, K of the beam center line by the relation

$$M = E\,I\,K \qquad [68]$$

where E is the modulus of elasticity of the beam material and I is the area moment of inertia around the neutral axis. This relation is derived from the basic assumption that plane sections remain plane after deformation, i.e. that the strain is given by[16]

$$\epsilon_x = z\,K = z\,\frac{\partial^2 w}{\partial x^2} \qquad [69]$$

where Z is the distance from the center line to any fiber within the depth of the beam. Thus the bending moment is given by

$$M = \int_A b(x,z)\ \sigma_x\ z\,dz \qquad [70]$$

where b(x,z) is the width of the beam (which could be a function of the depth (z) and the longitudinal dimension (x). For a rectangular beam of constant section (width 2B and depth 2H)

$$M = 2B\int_{-H}^{+H} \sigma_x \, z \, dz \qquad [71]$$

but

$$\sigma_x = E\,\epsilon_x = E\,z\,\frac{\partial^2 w}{\partial x^2} \qquad [72]$$

Thus

$$M = \frac{4}{3}\,E\,B\,H^3\frac{\partial^2 w}{\partial x^2} = E\,I\,\frac{\partial^2 w}{\partial x^2} \quad \text{where } I = \frac{4}{3}\,B\,H^3 \qquad [73]$$

In the theory of perfectly plastic solids[16] the perfectly plastic moment, M_o, is defined as the bending moment obtained when the cross section of the beam is entirely in the plastic region, thus for a rectangular beam[16]

$$M_o = 4B\int_0^H \sigma_y \, z \, dz = 2B\,\sigma_y\,H^2 \qquad [74]$$

where σ_0 is the yield stress of the material in pure tension. The moment curvature relation for an elastic-perfectly plastic solid rectangular beam will then be as shown in Figure 10.

If the Bell theory is employed then we must concern ourselves with the three regions enumerated by Bell.[6] For a rectangular beam it is found that

by letting $K = \frac{\partial^2 w}{\partial x^2}$ and $\epsilon = KH$, the strain at the outer fiber z=H

a. For $\epsilon < \epsilon_y$

$$M = 4B\int_0^H z^2\,E\,K\,dz \qquad \text{So} \quad \frac{M}{B\,H^2\,\sigma_y} = \frac{4}{3}\,\frac{E}{\sigma_y}\,\epsilon$$

[75]

b. For $\epsilon_y \leq \epsilon \leq \epsilon_c$

$$M = 4B\left\{\int_0^{\frac{\epsilon_y}{K}} \frac{\sigma_y z^2}{\frac{\epsilon_y}{K}}\,dz + \int_{\frac{\epsilon_y}{K}}^{H} z\left[\sigma_y + C\left(Kz - \epsilon_y\right)^{\frac{1}{2}}\right]dz\right\}$$

So

$$\frac{M}{B\,H^2\,\sigma_y} = 4\left[\frac{1}{3}\left(\frac{\epsilon_y}{\epsilon}\right)^2 + \frac{1}{2}\left(1 - \left(\frac{\epsilon_y}{\epsilon}\right)^2\right) + \frac{2C\left(2\epsilon_y + 3\epsilon\right)\left(\epsilon - \epsilon_y\right)^{3/2}}{15\,\epsilon^2\sigma_y}\right]$$

c. For $\epsilon > \epsilon_c$

$$M = 4B \left\{ \int_0^{\frac{\epsilon_y}{K}} \frac{\sigma_y z^2 \, dz}{\frac{\epsilon_y}{K}} + \int_{\frac{\epsilon_y}{K}}^{\frac{\epsilon_c}{K}} z \left[\sigma_y + C(K z - \epsilon_y)^{\frac{1}{2}} \right] dz + \int_{\frac{\epsilon_c}{K}}^{H} z \, C \, (Kz - \bar{\epsilon}_c)^{\frac{1}{2}} \, dz \right\}$$

$$\frac{M}{B H^2 \sigma_y} = 4 \left\{ \frac{1}{3} \left(\frac{\epsilon_y}{\epsilon}\right)^2 + \frac{1}{2} \left(\frac{\epsilon_c^2 - \epsilon_y^2}{\epsilon^2} \right) + \frac{2 C (2 \epsilon_y + 3 \epsilon_c) (\epsilon_c - \epsilon_y)^{3/2}}{15 \epsilon^2 \sigma_y} + \frac{2 C (2 \bar{\epsilon}_c + 3 \epsilon) (\epsilon - \bar{\epsilon}_c)^{3/2}}{15 \epsilon^2 \sigma_y} - \frac{2 C (2 \bar{\epsilon}_c + 3 \epsilon_c) (\epsilon_c - \bar{\epsilon}_c)^{3/2}}{15 \epsilon^2 \sigma_y} \right\}$$

where $\bar{\epsilon}_c = \epsilon_c - \epsilon_{N} / \lambda_N$

$$C = \lambda_N^{3/2} \, \bar{m}^{3/2} \, \beta_s$$

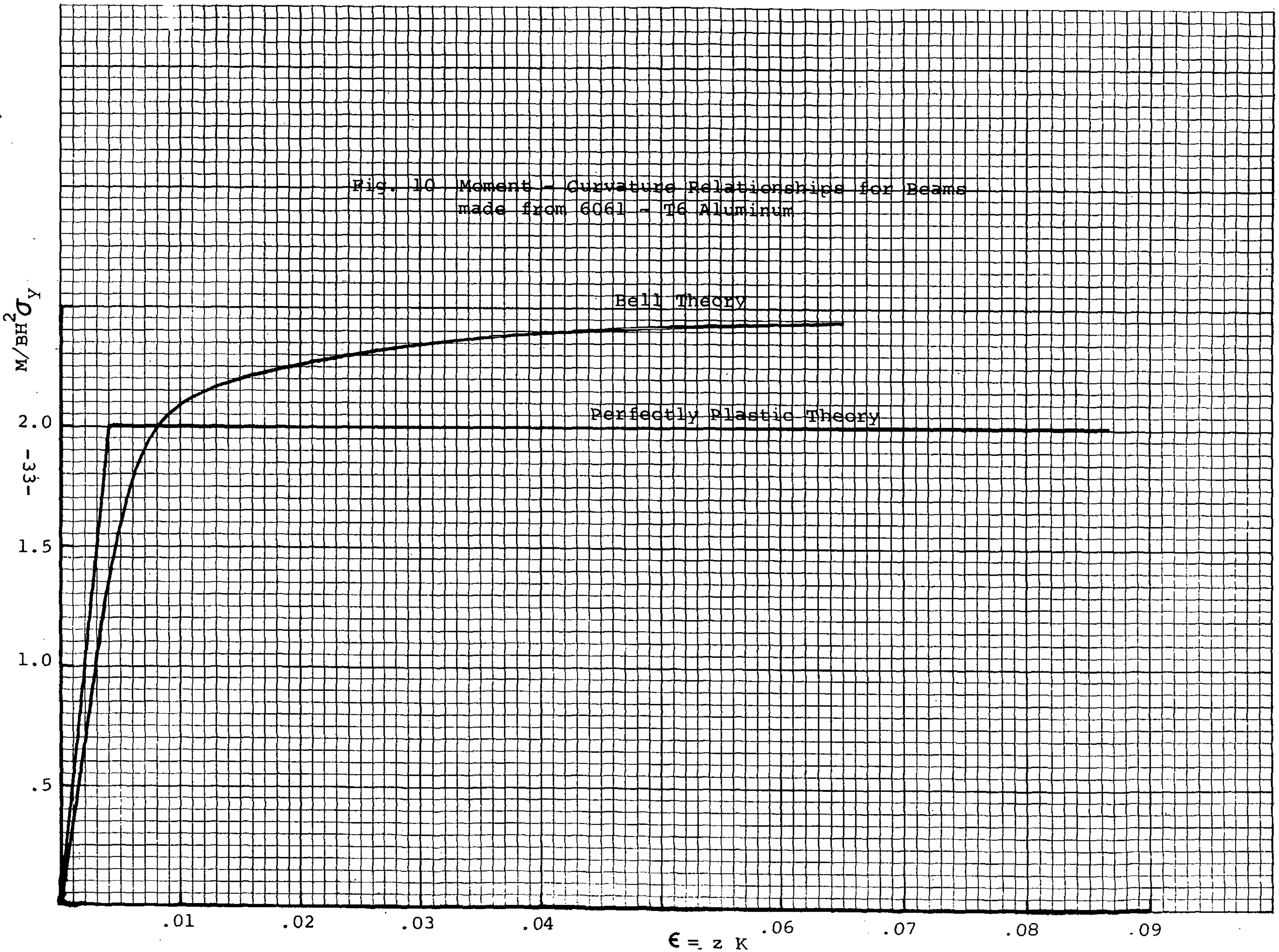

Fig. 10 Moment - Curvature Relationships for Beams made from 6061 - T6 Aluminum

The moment curvature relation as predicted by the elastic-perfectly plastic theory is compared to that predicted by the Bell theory for 6061-T6 aluminum in Figure 10. Note the smooth transition predicted by the Bell theory from the elastic through the elastic-plastic regions and finally into the completely plastic regime.

2. Calculation of energy absorbed in elastic-plastic deformation of beams

The elastic energy absorbed in the bending deformation of beams can be written as[5]

$$U_e = \int_0^L \frac{M^2}{2\,E\,I}\,dx \qquad [76]$$

where M is the elastic moment, E the elastic modulus, I the moment of inertia and L the beam length. For a rigid plastic material the plastic energy absorbed can be written[5]

$$U_p = \int_0^L M_o \frac{\partial^2 w}{\partial x^2}\,dx \qquad [77]$$

For an elastic-plastic material such as dealt with in the Bell Law the energy absorbed is given by[17]

$$U = \int_V \left[\int_0^{\epsilon_m} \sigma\, d\epsilon \right] dV^{*} \qquad [78]$$

but

$$\epsilon = z\,K \qquad d\epsilon = z\,dK \qquad [79]$$

so

$$U = \int_0^L dx \int_0^{(zK)_{max}} dK \; 4B \int_0^H \sigma\, z\, dz = \int_0^L dx \int_0^{(zK)_{max}} M(K)\, dK \qquad [80]$$

If we consider the case of a simply supported beam (i.e. one where the bending moment and deflection are both zero at the ends of the beam) and assume a deflection pattern as follows:

$$w = w_o \frac{16}{5} \frac{x}{L^4} \left(L^3 - 2\,L\,x^2 + x^3 \right) \qquad [81]$$

(this corresponds to the deflection pattern under a uniform load) then the energy can be computed as a function of w_o/L (w_o being the maximum center deflection of the beam and L being the length of the beam).

Figure 11 gives the results of this energy calculation. A sixteen point Gauss Quadrature was used to calculate both integrals shown in eq. [80]. The computer program that was used to make these computations is shown in Appendix I of this report. Note that for small elastic deformations U varies as $(w_o/L)^2$ whereas for the larger w_o/L it varies linearly with w_o/L. This has very interesting and simplifying consequences in the variational equation as shown in Section IVB. The results obtained by Westine and Baker[5] for the rigid - perfectly plastic material are also shown in Figure 11.

---

* where V denotes an integral over volume and ϵ_m is the maximum strain

Fig. 11 Energy Absorbed in 6061 - T6 Aluminum
Simply - Supported Beams

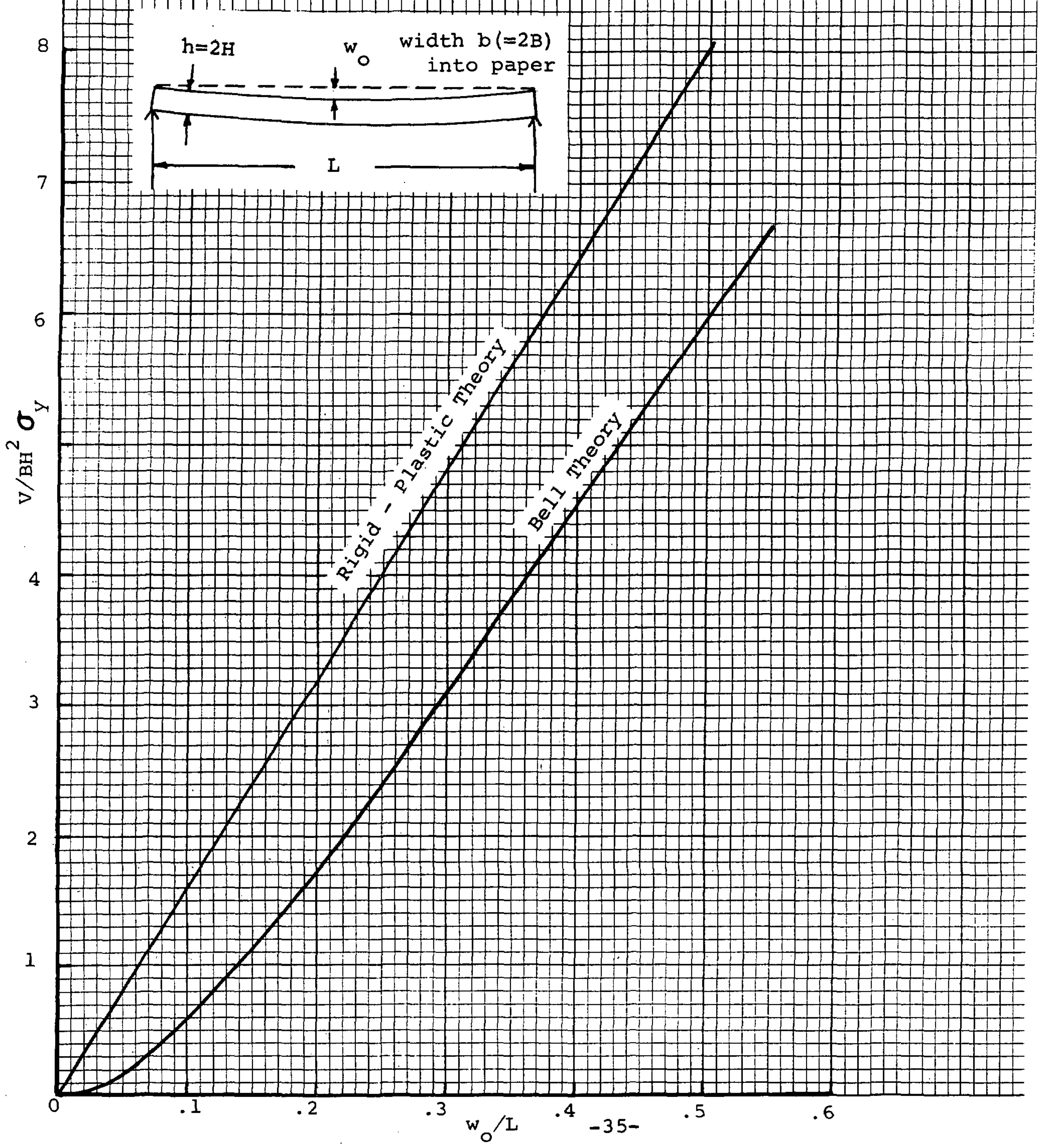

3. Calculation of permanent sets under impulsive loading

The total deflection (not the permanent set) of the beam under an impulsive load can be computed by the relation given in Section IV, i.e.

$$W_{P_e} = \frac{H_{m_e}^2}{2\, m_e}$$

$$\text{where } H_{m_e} = \int_0^T P_e(t)\, dt \quad \text{(the generalized impulse)}$$

$$m_e = \int_A \mu\, f_w^2(A)\, dA \quad \text{(the generalized mass)} \qquad [82]$$

$$W_{P_e} = U = \text{energy absorbed} \quad (\text{ a function of } w_o/L \text{ })$$

The program given in Appendix I is used to perform this computation. The results for the simply supported beam using the Bell Theory to compute the energy absorption are shown in Figure 12. The permanent set for a given impulse is computed as follows:

a. For a given value of impulse in Figure 13 pick off the value of w_o/L (this corresponds to the total deflection)

b. Compute the maximum strain in the center of the beam as a function of the center deflection (this curve is plotted in Fig. 14). At a given (w_o/L) center there is a corresponding value of (ϵ_m) center.

c. Go into the stress-strain curve of Figure 15 with this value of (ϵ_M) center and draw a line parallel to the elastic line at this strain. This corresponds to the unloading path from the maximum strain. Where the line hits the horizontal axis corresponds to the permanent strain.

d. Go back to the $W_o/L - \epsilon$ curve and obtain a corresponding value of W_o/L for this permanent strain. This will correspond to the permanent set (or permanent deflection).

e. Plot the impulse parameter originally chosen vs. this permanent set parameter as shown in Fig. 12.

Experimental points obtained from previous references[5,18] are shown on this plot. Indications are that this theory gives good results.

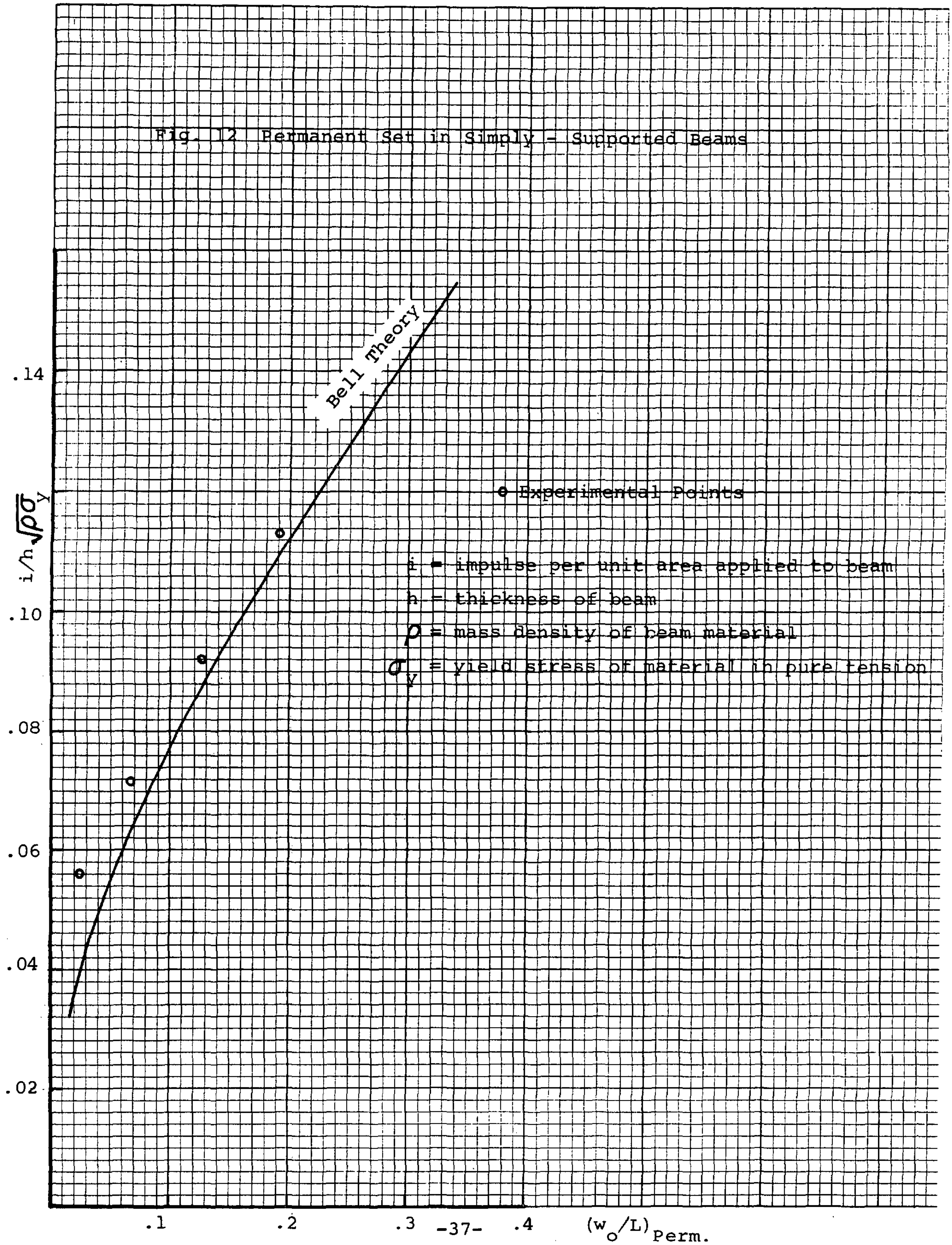

Fig. 12 Permanent Set in Simply - Supported Beams

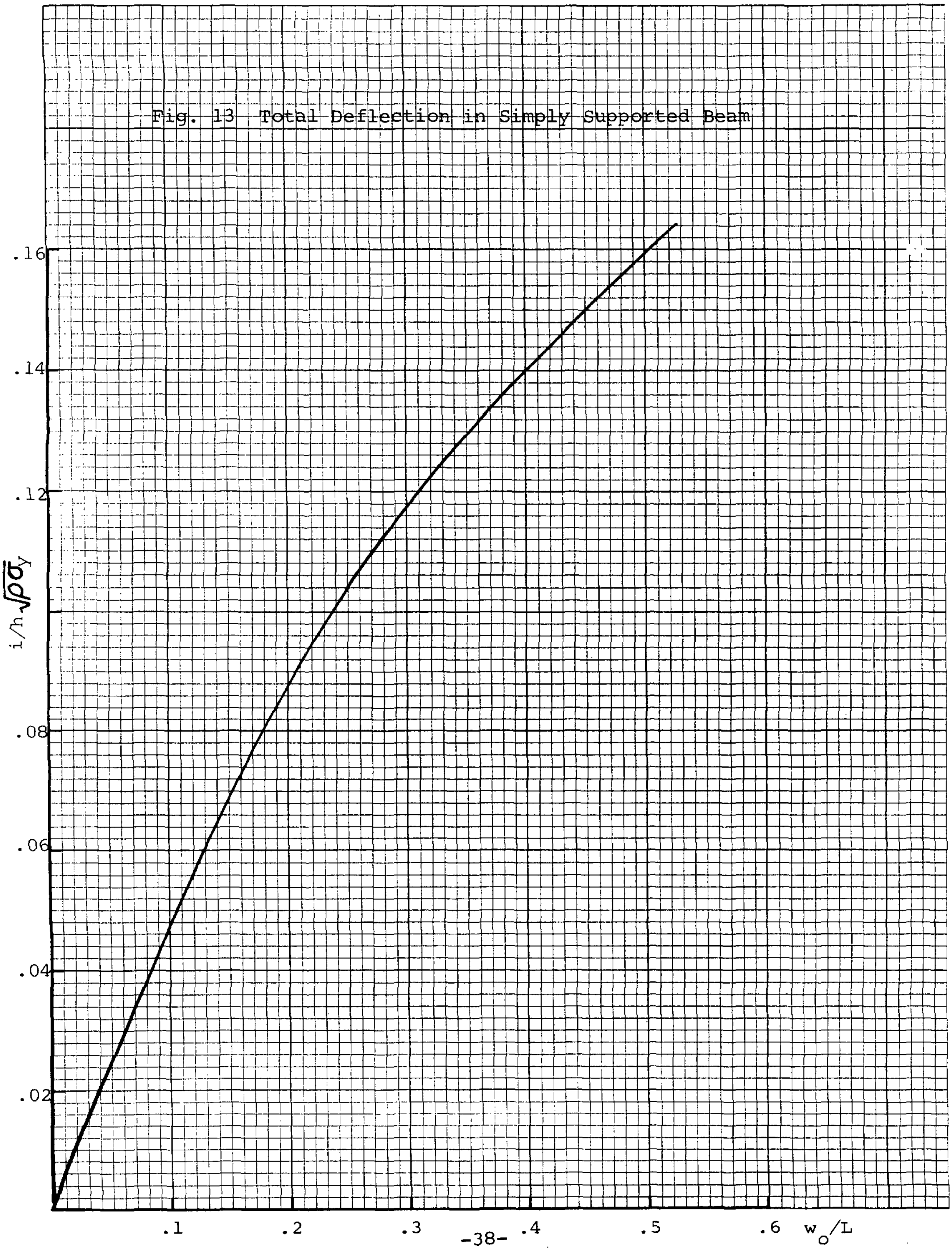

Fig. 13 Total Deflection in Simply Supported Beam

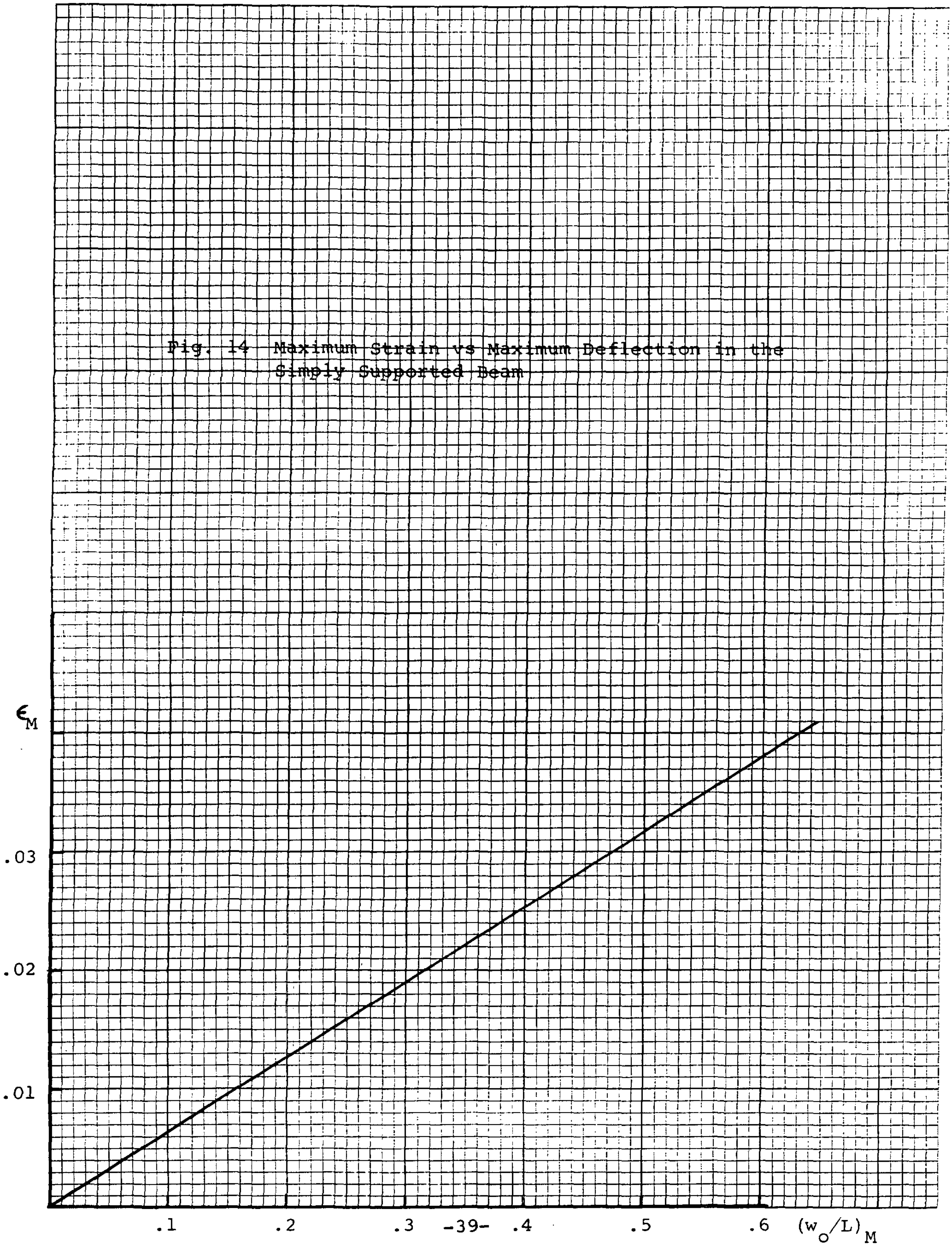

Fig. 14 Maximum Strain vs Maximum Deflection in the Simply Supported Beam

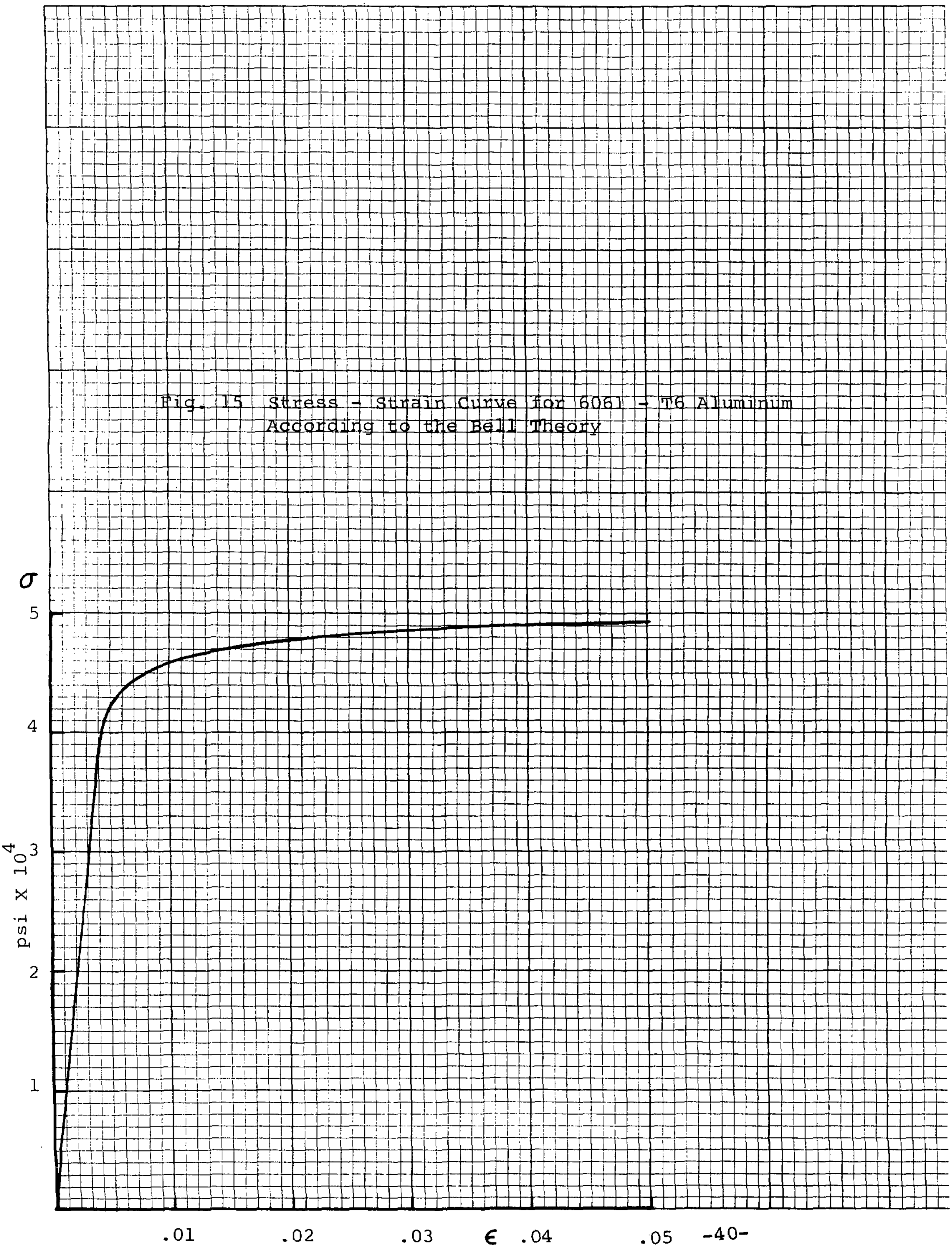

Fig. 15 Stress - Strain Curve for 6061 - T6 Aluminum According to the Bell Theory

C. Applications to two dimensional problems - bending and stretching of plates

Problems concerning the plastic deformation of plates involve biaxial stress fields and are therefore an order of magnitude more complicated to solve than one dimensional problems. However the employment of the Bell Theory readily enables solutions to be developed. The strain energy for a plate in a biaxial state of stress can be written[17]

$$U = \int_V \left[\int_0^{\Gamma_m} T \, d\Gamma \right] dV \qquad [83]$$

where V denotes an integral over volume

where

$$T = \sqrt{\tfrac{2}{3}} \sqrt{\sigma_X^2 + \sigma_Y^2 - \sigma_X\sigma_Y + 3\tau_{XY}^2} = \text{octahedral shear stress}$$

$$\Gamma = \sqrt{2}\sqrt{\epsilon_X^2 + \epsilon_Y^2 + \epsilon_X\epsilon_Y + \frac{\gamma_{XY}^2}{4}} = \text{octahedral shear strain} \qquad [84]$$

Γ_m = maximum value of Γ

$\sigma_X \ \sigma_Y \ \tau_{XY}$ = stress components , $\epsilon_X \ \epsilon_Y \ \gamma_{XY}$ = strain components

For a plate whose width, length and thickness are a, b 2H respectively the strain energy becomes

$$U = \int_0^a dx \int_0^b dy \int_{-H}^{+H} dz \int_0^{\Gamma_m} T \, d\Gamma \qquad [85]$$

Now introducing the Bell Law for biaxial stress, we have

$$T = E\Gamma \quad \text{for} \quad \Gamma < \Gamma_y$$

$$= T_y + \bar{c}\sqrt{\Gamma - \Gamma_y} \quad \text{for} \quad \Gamma_y \leqslant \Gamma \leqslant \Gamma_c \qquad \bar{c} = \lambda_N^{3/2} \bar{K}^{3/2} \beta_s \qquad [86]$$

$$= \bar{c}\sqrt{\Gamma - \bar{\Gamma}_c} \quad \text{for} \quad \Gamma > \Gamma_c \qquad \bar{\Gamma}_c = \Gamma_c - \Gamma_N/\lambda_N$$

For large lateral deformations of plates the strains can be written in terms of the lateral deflection, w, as follows:

$$\epsilon_x = \frac{1}{2}\left(\frac{\partial w}{\partial x}\right)^2 - z\frac{\partial^2 w}{\partial x^2} \qquad [87]$$

$$\epsilon_y = \frac{1}{2}\left(\frac{\partial w}{\partial y}\right)^2 - z\frac{\partial^2 w}{\partial y^2} \qquad \gamma_{xy} = \frac{\partial w}{\partial x}\frac{\partial w}{\partial y} - 2z\frac{\partial^2 w}{\partial x \, \partial y}$$

Now introduce a deflection function f(x,y) such that

$$w = w_o \, f(x,y) \qquad [88]$$

where f(x,y) is a nondimensional distribution function. Also nondimensionalize the other parameters as follows:

$$\bar{x} = x/a \, , \qquad \bar{y} = y/b \, , \qquad \bar{z} = z/H \, , \qquad \bar{\Gamma} = \Gamma / \Gamma_m \qquad [89]$$

So that[2] the strains become

$$\epsilon_x = \frac{1}{2} \frac{w_o^2}{a^2} \left(\frac{\partial f}{\partial \bar{x}} \right)^2 - \frac{z}{a} \frac{w_o}{a} \frac{\partial^2 f}{\partial \bar{x}^2} \qquad \gamma_{xy} = \frac{w_o}{a} \frac{w_o}{b} \left(\frac{\partial f}{\partial \bar{x}} \right) \left(\frac{\partial f}{\partial \bar{y}} \right)$$

$$\epsilon_y = \frac{1}{2} \frac{w_o^2}{b^2} \left(\frac{\partial f}{\partial \bar{y}} \right)^2 - \frac{z}{a} \frac{w_o}{b} \frac{\partial^2 f}{\partial \bar{y}^2} \qquad - 2 \frac{z \, w_o}{a \, b} \frac{\partial^2 f}{\partial \bar{x} \, \partial \bar{y}} \qquad [90]$$

The strain energy becomes

$$U = a \, b \, H \, E \left[\int_0^1 d\bar{x} \int_0^1 d\bar{y} \int_{-1}^{+1} d\bar{z} \int_0^1 T \, \Gamma_m \, d\bar{\Gamma} \right] \qquad [91]$$

Now assume that the edges of the plate are simply supported and let the deflection function be given as[5]

$$f(x,y) = \frac{1}{4} \left(1 + \cos \left[\frac{\pi \left(x - \frac{a}{2} \right)}{\frac{a}{2}} \right] \right) \left(1 + \cos \left[\frac{\pi \left(y - \frac{b}{2} \right)}{\frac{b}{2}} \right] \right) \qquad [92]$$

or in terms of $\bar{x}$, $\bar{y}$

$$f(\bar{x},\bar{y}) = \frac{1}{4} \left(1 + \cos \pi (2\bar{x} - 1) \right) \left(1 + \cos \pi (2\bar{y} - 1) \right) \qquad [93]$$

The program for computing the energy integral is contained in Appendix 2. A plot of the strain energy as a function of the deflection resulting from calculations using the program is shown in Figure 16. Assuming impulsive loading and equating the kinetic energy to the strain energy (no corrections are made for the shape function as done for the beam since the correction is small for the simply supported case) we can then obtain a relationship between the nondimensional impulse function and the nondimensional deflection. This curve is shown in Fig. 17. Using an analogous procedure for obtaining permanent set as was used for beams we go through the following steps:

a. Plot a curve of nondimensional impulse vs. nondimensional total deflection such as shown in Fig. 17

b. Plot a curve of octahedral shear strain, Γ vs. nondimensional deflection w_o/h such as shown in Fig. 18. For the given value of w_o/h from a, we have a value for Γ

c. Go into the stress-strain curve ($T - \Gamma$) in Figure 19 and obtain the permanent strain by drawing a line parallel to the elastic line at the strain which corresponds to the appropriate value of w_o/h.

d. Go back to Figure 18 to obtain the permanent set value of w_o/h and plot on Figure 17.

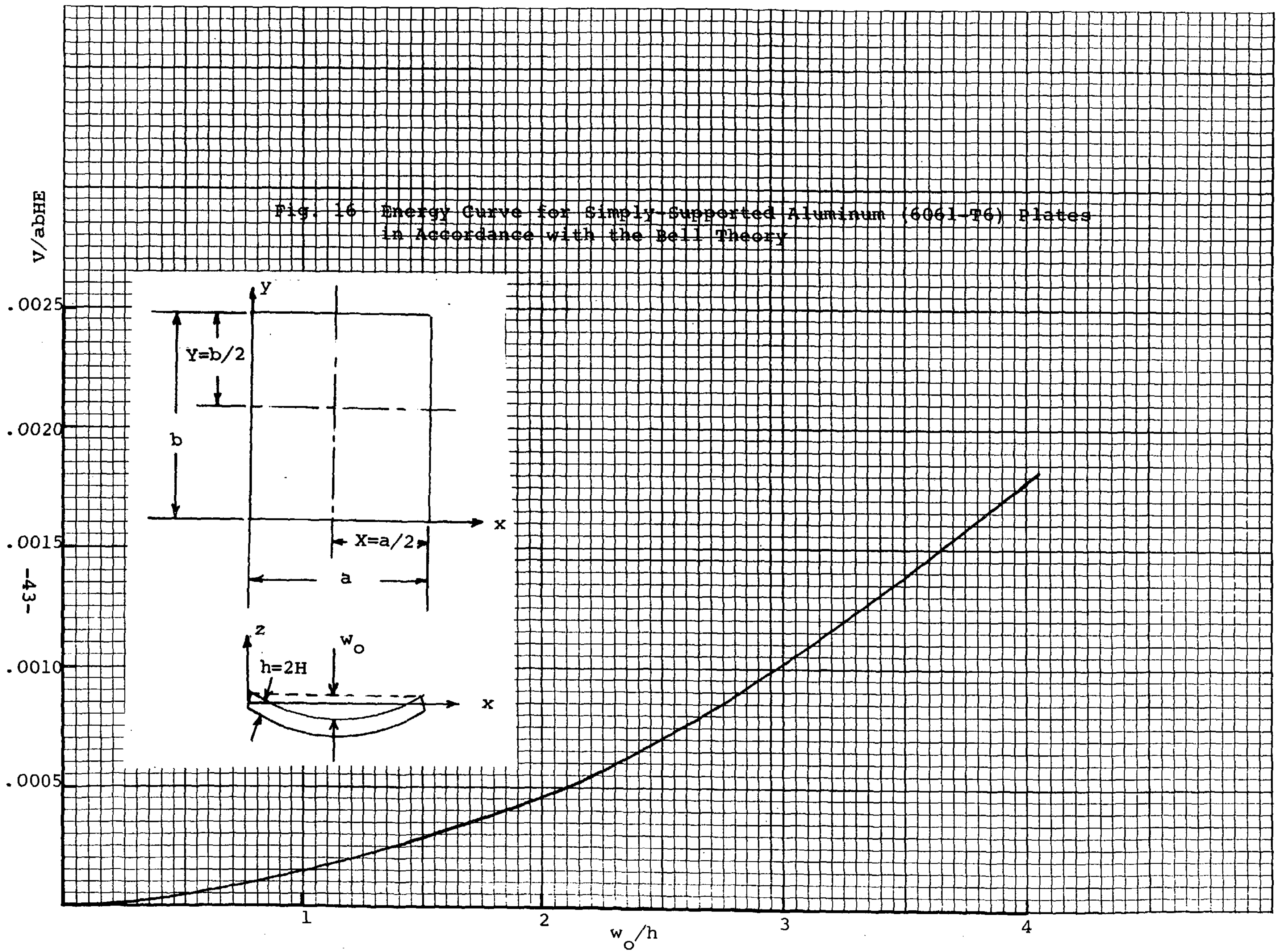

Fig. 16 Energy Curve for Simply-Supported Aluminum (6061-T6) Plates in Accordance with the Bell Theory

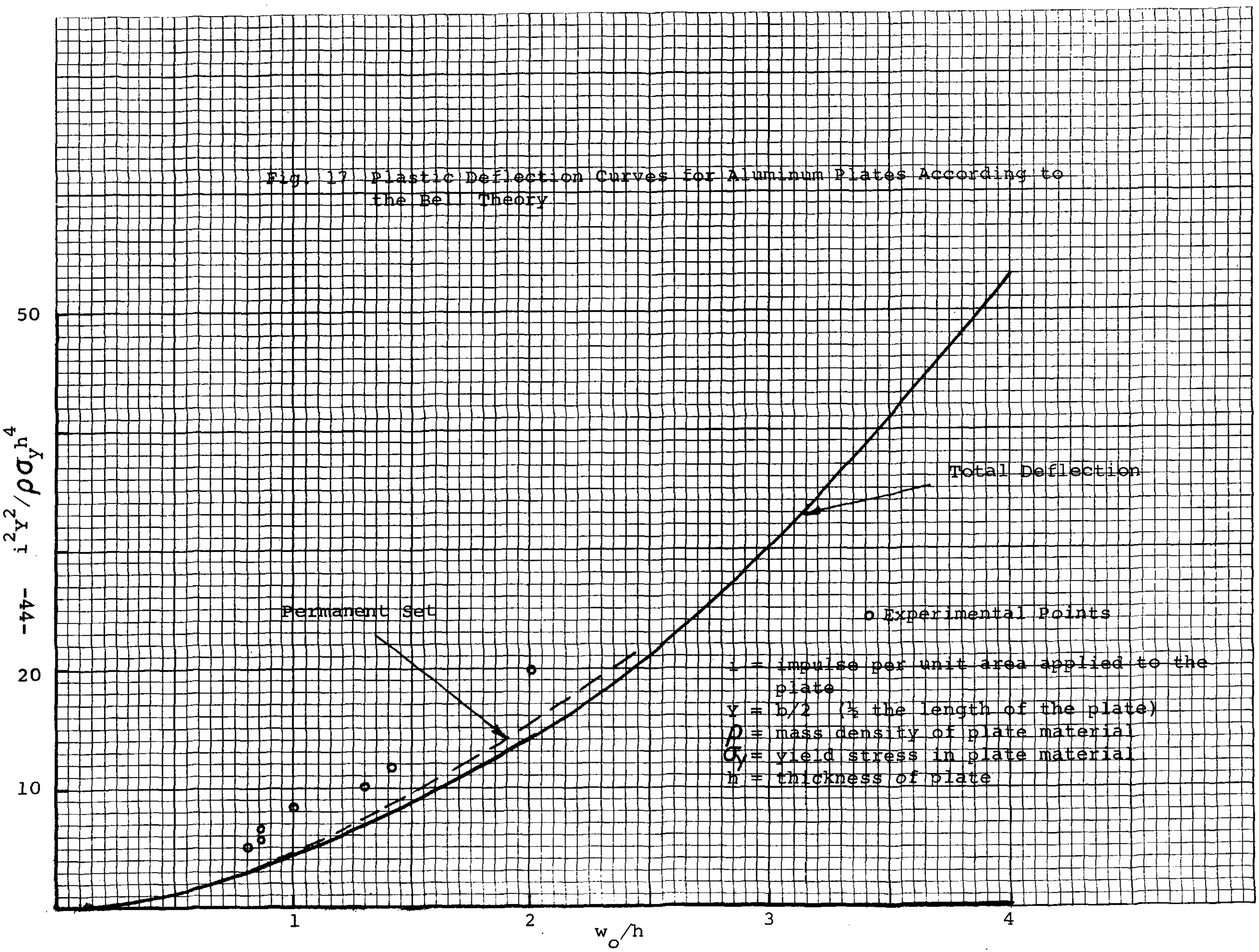

Fig. 17 Plastic Deflection Curves for Aluminum Plates According to the Bell Theory

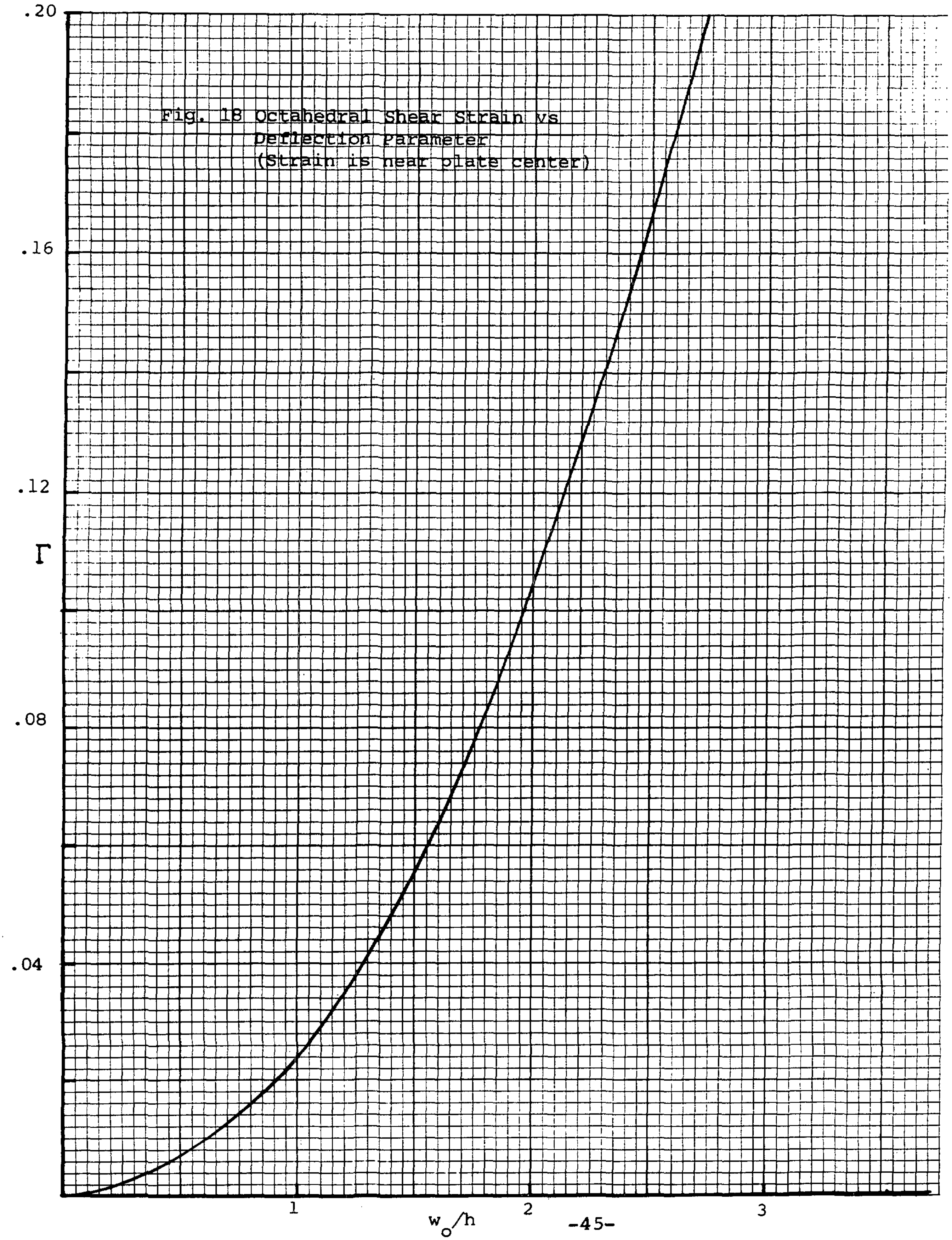

Fig. 18 Octahedral Shear Strain vs
Deflection Parameter
(Strain is near plate center)

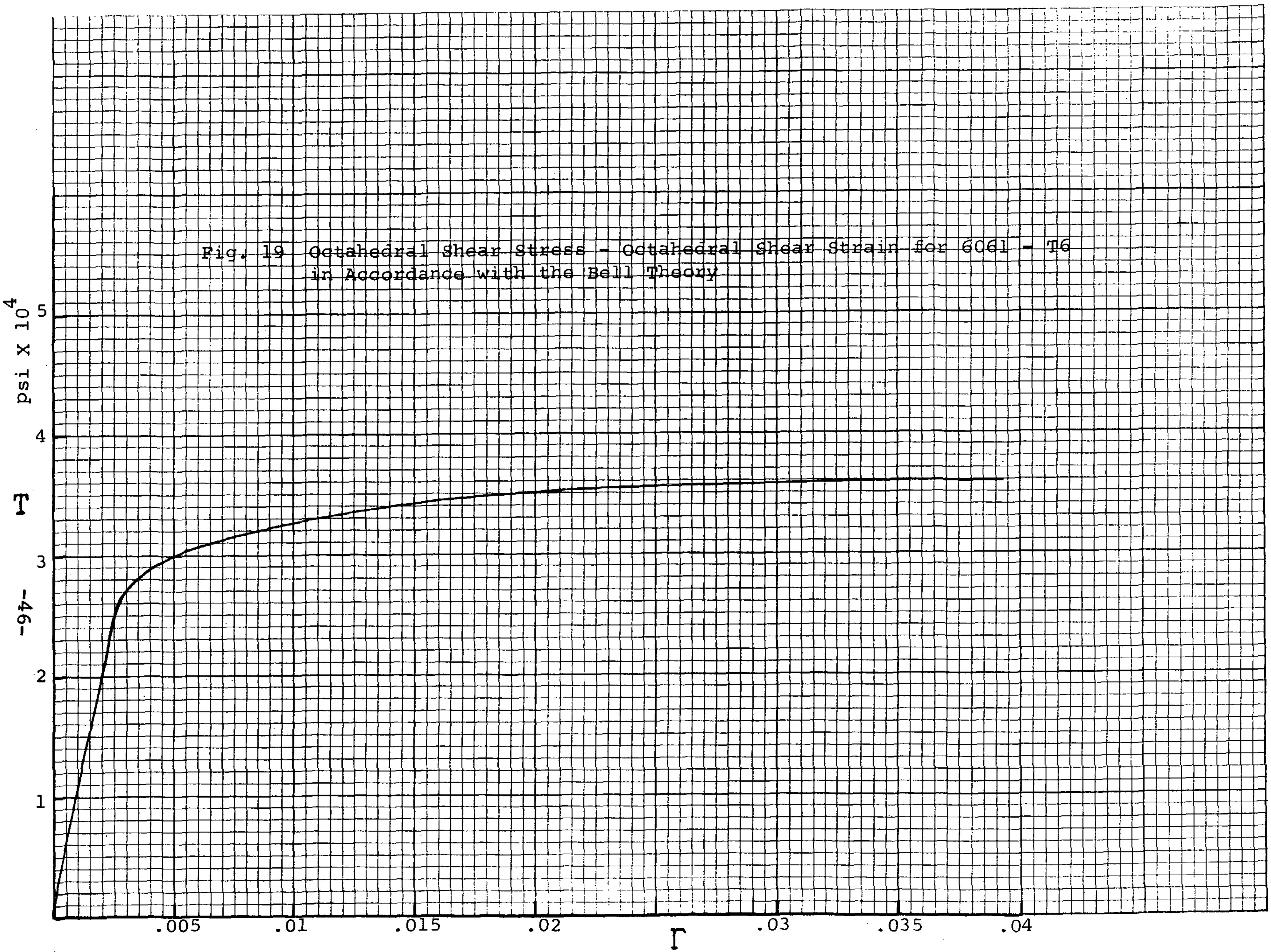

Fig. 19 Octahedral Shear Stress - Octahedral Shear Strain for 6061 - T6 in Accordance with the Bell Theory

Both the nondimensional impulse - deflection values for total deflection and permanent set are shown in Figure 17 with corresponding experimental results obtained from the literature.[5,19] The indications are that the theory is quite satisfactory in predicting plastic deflections.

D. Bell's theory and the variational method

Once the energy function is computed, a polynomial fit can be made between energy and deflection. For example, in the case of a simply supported plate shown in Fig. 16 the energy takes the form

$$\frac{V}{a\ b\ H\ E} = A\left(\frac{w_o}{h}\right) + B\left(\frac{w_o}{h}\right)^2 \qquad [94]$$

where $A = .0009$, $B = .0008$

These coefficients are somewhat less than those computed from the rigid-perfectly plastic theory presented by Westine and Baker.[5] In any event if a second order polynomial will fit the energy function then all the theory developed in section IV C can be applied to the problem up to the point of predicting the complete isodamage curve.

A practical way to apply the Bell Theory to dynamic problems in plates and shells is first to compute the energy, fit a polynomial in the deflection to this energy function and then apply the variational theory outlined in the earlier sections of this report.

E. Possibilities for other applications of the Bell theory

The problems presented in this section are only a small example of the application of Bell's theory to dynamic vulnerability type problems. There are many unsolved vulnerability problems to which the new Bell laws could be applied to shed light on their solution. One very important problem is the penetration and perforation of structures by projectiles. These perforation problems have only been investigated either empirically or analytically using questionable stress-strain laws. Another problem of great interest is the dynamic behavior of shells. The solution of this problem should be merely an extension of the analysis presented for plates in this report.

APPENDIX I. COMPUTER PROGRAM FOR THE BEAM USING BELL'S LAW

A listing of the beam probram in "BASIC" is given in Table 1. The input parameters are shown in statements 10 - 45, 100 - 210 with their corresponding values given in the DATA statements 480 - 600. The input parameters in the program are given below with the symbols that they represent.

C = $\lambda_N^{3/2}\bar{m}^{3/2}\beta_s$ = 85000 psi

E1 = $\epsilon_c - \dfrac{\epsilon_N}{\lambda_N}$ = -.285

Y = ϵ_y = .004

S = σ_y = 40000 psi

E2 = ϵ_c = .01

E = elastic modulus = 10^7 psi

M = number of integration points for the $\bar{X}$ integral = 16

N = number of integration points for the K integral = 16

H = h/2L = one half the thickness of the beam divided by its length = .0069

W1, W2, W3 = minimum, maximum, increment in W where W = w_o/L in which w_o is the maximum deflection and L is the beam length

G1, G2, G3 = minimum, maximum, increment in G, where G is the strain value used to compute the stress-strain curve in statements 55-97.

X(I),G(I) are the Gauss locations and weights respectively for the x integration (locations are in statements 530 - 540, weights in statements 550-560)

Y(J), H(J) are Gauss locations and weights respectively for the K integration (locations are in statements 570-580, weights in 590-600)

U is the nondimensional energy function $V/BH^2\sigma_y$ as shown in the graph of Fig. 11

Table 1. Listing of Beam Program

```
5  DIM X(20),G(20),Y(20),H(20)
10  READ C,E1,Y,S,E2,E
20  READ M,N
30  READ H
40  READ W1,W2,W3
45  READ G1,G2,G3
50  LET Q= 0
55  FOR G=G1 TO G2 STEP G3
60  IF G>Y THEN 72
65  LET S5=E*C
70  GOTO 95
72  IF G>E2 THEN 90
75  LET S5=S+C*SQR(G-Y)
80  GOTO 95
90  LET S5=C*SQR(G-E1)
95  GOTO 97
97  NEXT C
100  FOR I= 0 TO M- 1
110  READ X(I)
120  NEXT I
130  FOR I= 0 TO M- 1
140  READ G(I)
150  NEXT I
160  FOR J= 0 TO N- 1
170  READ Y(J)
180  NEXT J
190  FOR J= 0 TO N- 1
200  READ H(J)
210  NEXT J
215  FOR W=W1 TO W2 STEP W3
220  FOR I= 0 TO M- 1
230  FOR J= 0 TO N- 1
240  LET F8=( 192/ 5)*(X(I)-X(I)↑ 2)
250  LET K=H*W*F8*Y(J)
260  IF K>Y THEN 290
270  LET B=( 4/ 3)*E*K/S
280  GOTO 410
290  LET A=(S/ 3)*(Y/K)↑ 2
300  IF K>E2 THEN 350
310  LET A1=(S/ 2)*( 1-(Y/K)↑ 2)
320  LET A2=( 2*C*( 2*Y+ 3*K)*(K-Y)↑ 1.5)/( 15*K↑ 2)
330  LET B= 4*(A+A1+A2)/S
340  GOTO 410
350  LET B3=(S/ 2)*((E2/K)↑ 2-(Y/K)↑ 2)
360  LET D3=( 2*C*( 2*Y+ 3*E2)*(E2-Y)↑ 1.5)/( 15*K↑ 2)
370  LET F1= 2*C*( 2*E1+ 3*K)*(K-E1)↑ 1.5
380  LET F2= 2*C*( 2*E1+ 3*E2)*(E2-E1)↑ 1.5
390  LET F=(F1-F2)/( 15*K↑ 2)
400  LET B= 4*(A+B3+D3+F)/S
410  LET Q=Q+G(I)*H(J)*F8*B
420  NEXT J
430  NEXT I
435  LET U=W*Q
440  PRINT W,U
460  LET Q= 0
470  NEXT W
```

Table 1 - Cont'd

```
480  DATA  85000,-.285
481  DATA  4.00000E-03, 40000, 1.00000E-02, 1.00000E+07
490  DATA  16, 16
500  DATA  6.90000E-03
520  DATA  5.00000E-02, .5, 5.00000E-02
521  DATA  1.00000E-03, 1.00000E-02, 1.00000E-03
530  DATA  5.29954E-03, 2.77124E-02, 6.71844E-02, .122297
532  DATA  .191061, .270991, .359198, .452493
535  DATA  .547506, .640801, .729008, .808938
540  DATA  .877702, .932815, .972287, .9947
550  DATA  1.35762E-02, 3.11267E-02, 4.75792E-02, 6.23144E-02
552  DATA  7.47980E-02, 8.45782E-02, 9.13017E-02, 9.47243E-02
555  DATA  9.47253E-02, 9.13017E-02, 8.45782E-02, 7.47980E-02
560  DATA  6.23144E-02, 4.75792E-02, 3.11267E-02, 1.35762E-02
570  DATA  5.29954E-03, 2.77124E-02, 6.71844E-02, .122297
572  DATA  .191061, .270991, .359198, .452493
575  DATA  .547506, .640801, .729008, .808938
580  DATA  .877702, .932815, .972287, .9947
590  DATA  1.35762E-02, 3.11267E-02, 4.75792E-02, 6.23144E-02
592  DATA  7.47980E-02, 8.45782E-02, 9.13017E-02, 9.47253E-02
595  DATA  9.47253E-02, 9.13017E-02, 8.45782E-02, 7.47980E-02
600  DATA  6.23144E-02, 4.75792E-02, 3.11267E-02, 1.35762E-02
700  END
```

APPENDIX II. COMPUTER PROGRAM FOR THE PLATE USING BELL'S LAW

A listing of the plate program in "BASIC" is given in Table 2. The input parameters are shown in statements 20 - 220 with their corresponding values given in the DATA statements 720 - 870. The input parameters in the program are given below with the symbols they represent:

C = $\lambda_N^{3/2} K^{-3/2} \beta_s$ = 60000 psi

E = elastic modulus = 10^7 psi

T1 = τ_y = 28000 psi

G1 = Γ_y = .0035

G2 = Γ_c = .013

G3 = $\Gamma_c - \Gamma_N/\lambda_N$ = -.33

S = σ_y = 40000 psi

M = number of integration points for x integral = 4

N = number of integration points for y integral = 4

P = number of integration points for z integral = 7

Q = number of integration points for Γ integral = 5

H = h/2a = one half the thickness of the plate divided by the width

A9 = a/b = width/length

W1,W2,W3 = minimum, maximum, increment in W where W = w_o/a (w_o = maximum deflection)

X(I),A(I) = locations, weights for x Gauss integration

Y(J),B(J) = locations, weights for y Gauss integration

Z(K),C(K) = locations, weights for z Bauss integration

G(L),D(L) = locations, weights for Γ integration

The nondimensional impulse function is given by I6 and the nondimensional deflection parameter w_o/h by W9. The nondimensional energy function V/abHE is given in the program by the symbol V.

Table 2. Listing of Plate Program

```
10   DIM X(10),Y(10),Z(10),G(10),A(10),B(10),C(10),D(10)
20   READ C,E,T1,G1,G2,G3,S
25   READ M,N,P,Q
30   READ H,A9
40   READ W1,W2,W3
50   FOR I= 0 TO M- 1
55   READ X(I)
60   NEXT I
65   FOR I= 0 TO M- 1
70   READ A(I)
75   NEXT I
80   FOR J= 0 TO N- 1
85   READ Y(J)
90   NEXT J
95   FOR J= 0 TO N- 1
100   READ B(J)
105   NEXT J
110   FOR K= 0 TO P- 1
120   READ Z(K)
130   NEXT K
140   FOR K= 0 TO P- 1
150   READ C(K)
160   NEXT K
170   FOR L= 0 TO Q- 1
180   READ G(L)
190   NEXT L
200   FOR L= 0 TO Q- 1
210   READ D(L)
220   NEXT L
295   LET V= 0
300   FOR W=W1 TO W2 STEP W3
310   FOR I= 0 TO M- 1
320   FOR J= 0 TO N- 1
350   LET X1= 3.14159*( 2*X(I)- 1)
360   LET Y1= 3.14159*( 2*Y(J)- 1)
370   LET F1= .25*(-6.28319*SIN(X1))*( 1+COS(Y1))
380   LET F2= .25*(-39.4784*COS(X1))*( 1+COS(Y1))
390   LET F3= .25*( 1+COS(X1))*(-6.28319*SIN(Y1))
400   LET F4= .25*( 1+COS(X1))*(-39.4784*COS(Y1))
410   LET F5= .25*(-6.28319*SIN(X1))*(-6.28319*SIN(Y1))
415   FOR K= 0 TO P- 1
420   LET E1= .5*(W↑ 2)*(F1↑ 2)-Z(K)*W*F2*H
430   LET E2= .5*(W↑ 2)*(A9↑ 2)*(F3↑ 2)-Z(K)*H*W*A9*F4
440   LET E3=W*W*A9*F1*F3- 2*Z(K)*H*W*A9*F5
450   LET G9= 1.41399*SQR((E1↑ 2)+(E2↑ 2)+(E1*E2)+ .25*(E3↑ 2))
460   FOR L= 0 TO Q- 1
470   LET G=G9*G(L)
480   IF G>G1 THEN 505
490   LET T=G
500   GOTO 540
505   IF G>G2 THEN 530
510   LET T=(T1/E)+(C/E)*SQR(G-G1)
520   GOTO 540
530   LET T=(C/E)*SQR(G-G3)
540   LET V=V+T*G9*A(I)*B(J)*C(K)*D(L)
```

Table 2 - Cont'd

```
550  NEXT L
560  NEXT K
570  NEXT J
580  NEXT I
590  LET I6= .25*( 1/(A9* 2*H)↑2)*(E/S)*V
600  LET W9= .5*W/H
700  PRINT I6,W9
710  LET V= 0
715  NEXT W
720  DATA  85000, 1.00000E+07, 35000, 5.00000E-03, 1.30000E-02,-.33, 40000
730  DATA  4, 4, 7, 5
740  DATA  4.00000E-02, .59
750  DATA  8.00000E-02, .8, 8.00000E-02
760  DATA  6.94318E-02, .330009, .66999, .930568
770  DATA  .173927, .326072, .326072, .173927
780  DATA  6.94318E-02, .330009, .66999, .930568
790  DATA  .173927, .326072, .326072, .173927
800  DATA -.949108,-.741531,-.405845, 0
810  DATA  .405845, .741531, .949108
820  DATA  .129484, .279705, .38183, .417959
830  DATA  .38183, .279705, .129484
840  DATA  4.69100E-02, .230765, .5
850  DATA  .769234, .95309
860  DATA  .118463, .239314, .284444
870  DATA  .239314, .118463
900  END
```

REFERENCES

1. James F. Bell, "The Experimental Foundations of Solid Mechanics," Encyclopedia of Physics, Vol. Vla/1, Mechanics of Solids I, Editor C. Truesdell, Springer Verlag, New York, 1973.

2. W. Prager and P. G. Hodge, Jr., "Theory of Perfectly Plastic Solids," John Wiley & Sons, Inc., New York, 1951.

3. R. Hill, "The Mathematical Theory of Plasticity," Oxford at the Clarendon Press, London, 1950.

4. N. Cristescu, "Dynamic Plasticity" John Wiley & Sons, Inc., New York, 1967.

5. P. S. Westine, and W. E. Baker, "Energy Solutions for Predicting Deformations in Blast Loaded Structures," Southwest Research Institute, presented at the 16th Explosive Safety Seminar, Hollywood Beach, Fla., Sept., 1974.

6. James F. Bell, "A New, General Theory of Plasticity for Structural Metal Alloys," The Johns Hopkins University, Final Report on Contract No. DAAD05-70-C-0054 for U. S. Army Ballistics Research Laboratories, Aberdeen Proving Ground, Maryland, May, 1975.

7. J. E. Greenspon, "Some Basic Principles for Damage to Structures by Fragments and Blast," J G Engineering Research Associates, BRL CR 96 prepared for Ballistic Research Laboratories, Aberdeen Proving Ground under Contract DAAD05-72-C-0195, March, 1973. AD #909896L.

8. J. E. Greenspon, "Elastic-Plastic Response of Structures to Blast and Impulse Loads," JG ENGINEERING RESEARCH ASSOCIATES, Contract DA-18-001-AMC-1019(X) for Ballistic Research Laboratories, Aberdeen Proving Ground, Maryland, Tech. Rep. No. 7, March, 1967.

9. J. E. Greenspon, "Theoretical Calculation of Isodamage Characteristics," J G ENGINEERING RESEARCH ASSOCIATES, Contract DAAD05-69-C-0116 for Ballistic Research Laboratories, Aberdeen Proving Ground, Maryland, Tech. Rep. No. 10, Feb., 1970.

10. J. E. Greenspon, "Some Work-Energy and Variational Principles Applied to Blast Loading of Structures," J G ENGINEERING RES. ASSOC., Contract DAAD 05-67-C-0331 for Ballistic Research Laboratories, Aberdeen Proving Ground, Md., Tech. Rep. No. 9, Oct., 1968.

11. J. E. Greenspon, "Damage to Structures by Fragments and Blast," J G ENGINEERING RESEARCH ASSOCIATES, Contract DAAD05-70-C-0194 for Ballistic Research Labs., Aberdeen Proving Ground, Md. Tech Rep. No. B-11, June, 1971.

12. Ballistic Analysis Laboratory, The Johns Hopkins University, "The Resistance of Various Metallic Materials to Perforation by Steel Fragments; Empirical Relationships for Fragment Residual Velocity and Residual Weight," Baltimore, Md., Institute for Cooperative Research, BAL/JHU, April, 1961 (Project THOR Tech. Rep. No. 47).

13. J. E. Greenspon, "Collapse, Buckling and Post Failure Behavior of Cylindrical Shells Under Elevated Temperature and Dynamic Loads," J G ENG. RES. ASSOC., Contract DA-18-001-AMC-707(X) for Ballistic Research Labs., Aberdeen Prov. Ground, Md., Tech. Rep. No. 6, Nov., 1965.

14. W. E. Baker, W. O. Ewing, Jr., J. W. Hanna and G. E. Bunnewith "The Elastic and Plastic Response of Cantilevers to Air Blast Loading,"BRL Rep. No. 1121, Dec., 1960, (Ballistic Research Labs., Aberdeen Proving Ground, Md.). AD #252542.

15. C. H. Norris, R. J. Hansen, M. J. Holley, Jr., J. M. Biggs, S. Namyet, J. K. Minami, "Structural Design for Dynamic Loads," McGraw Hill Book Co., Inc., New York, 1959, p. 135-346.

16. P. G. Hodge, Jr., "Plastic Analysis of Structures," McGraw Hill Book Co., Inc., New York, 1959, p. 10 - 11.

17. Iliouchine, "Plasticite," (Translated from the original Russian into French), Edition Eyrolles, 1956.

18. A. L. Florence and R. D. Firth, "Rigid - Plastic Beams Under Uniformly Distributed Impulses," J. Appl. Mech., 32, Series E,1, March, 1965.

19. N. Jones, T. O. Uran, and S. A. Tekin, "The Dynamic Plastic Behavior of Fully Clamped Rectangular Plates," Int. Jour. Solids and Structures, 6, 1970, pp. 1499 - 1512.

ACKNOWLEDGEMENTS

This work was sponsored by the U.S.A. Ballistic Research Laboratories at Aberdeen Proving Ground. The author would like to express his deepest appreciation to Mr. O. T. Johnson, the technical supervisor of the project, for his continuing guidance and encouragement.

DISTRIBUTION LIST

No. of Copies	Organization
12	Commander Defense Documentation Center ATTN: DDC-TCA Cameron Station Alexandria, VA 22314
1	Director Defense Advanced Research Projects Agency 1400 Wilson Boulevard Arlington, VA 22209
2	Director Weapons System Evaluation Group Washington, DC 20305
3	Director Defense Intelligence Agency ATTN: DI-7B, R. Sauer W. B. Neal DI-2C, L. Bradley Washington, DC 20301
1	Assistant Secretary of Defense (SA) ATTN: Dr. M. Bailey Washington, DC 20301
1	Commander US Army Materiel Development and Readiness Command ATTN: DRCDMA-ST 5001 Eisenhower Avenue Alexandria, VA 22333
1	Commander US Army Materiel Development and Readiness Command ATTN: DRCDE-D 5001 Eisenhower Avenue Alexandria, VA 22333
1	Commander US Army Materiel Development and Readiness Command ATTN: DRCCP 5001 Eisenhower Avenue Alexandria, VA 22333
4	Commander US Army Aviation Systems Command ATTN: DRSAV-E DRSAV-ERP DRSAV-EFI, G. Kovacs DRSAV-ERS, J. Poynton 12th and Spruce Streets St. Louis, MO 63166
3	Commander US Army Aviation Systems Command ATTN: DRCPM-HL, R. Johnson DRCPM-ASE, E. Branhof DRCPM-AAH-TM, C. Vark 12th and Spruce Streets St. Louis, MO 63166
1	Director US Army Air Mobility Research and Development Laboratories Ames Research Center Moffett Field, CA 94035
4	Commander US Army Air Mobility Research and Development Laboratory ATTN: SAVDL-EU-PP, Mr. Morrow SAVDL-EU-SS, Mr. Robinson SAVDL-EU-RM SAVDL-EU-SS, Mr. Merritt Fort Eustis, VA 23604
1	Commander US Army Electronics Command ATTN: DRSEL-RD Fort Monmouth, NJ 07703

DISTRIBUTION LIST

No. of Copies	Organization
3	Commander US Army Missile Command ATTN: DRSMI-R DRSMI-CM DRSMI-RFG D. R. Peterson Redstone Arsenal, AL 35809
3	Commander US Army Missile Command ATTN: DRCPM-MDEI-PA DRCPM-HA DRCPM-SHO-E Redstone Arsenal, AL 35809
1	Commander US Army Tank Automotive Logistics Command ATTN: DRSTA-RHFL Warren, MI 48090
2	Commander US Army Mobility Equipment Research & Development Command ATTN: Tech Docu Cen, Bldg 315 DRSME-RZT Fort Belvoir, VA 22060
1	Commander US Army Armament Command Rock Island, IL 61202
3	Commander US Army Picatinny Arsenal ATTN: SARPA-AP SARPA-DW8 SARPA-AD-C-S Mr. Turoczy Dover, NJ 07801
1	President US Army Aviation Test Board Fort Rucker, AL 36360
1	President US Army Infantry Board Fort Benning, GA 31905
1	Commander US Army Harry Diamond Laboratories ATTN: DRXDO-TI 2800 Powder Mill Road Adelphi, MD 20783
1	Director US Army Material and Mechanics Research Center ATTN: DRXMR-ATL Watertown, MA 02172
1	Commander US Army Natick Research and Development Command ATTN: DRXRD, Dr. D. Sieling Natick, MA 01760
2	Commander US Army Foreign Science and Technology Center Federal Office Building ATTN: DRXST-CV, Mr. Petrie Mr. J. Ward, Jr. 220 7th Street, NE Charlottesville, VA 22901
1	Commander US Army Training and Doctrine Command ATTN: ATCD-CS-M-AR Fort Monroe, VA 22060
1	Commander US Army TRADOC Systems Analysis Activity ATTN: ATAA-SA White Sands Missile Range NM 88002

DISTRIBUTION LIST

No. of Copies	Organization
1	Commander US Army Experimentation Command ATTN: CSCG Ln Office Fort Ord, CA 93941
1	Commandant US Army Transportation Corps School Fort Eustis, VA 23604
1	Commander US Army Infantry School ATTN: Infantry Agency Fort Benning, GA 31905
1	Commandant US Army Aviation School Fort Rucker, AL 36360
1	Commandant US Army Armor School ATTN: Armor Agency Fort Knox, KY 40121
2	Commander US Army Agency for Aviation Safety Fort Rucker, AL 36360
1	HQDA (DAMA-AR) Washington, DC 20310
1	HQDA (DAMA-ZA) Washington, DC 20310
1	HQDA (SAUS-OR) Washington, DC 20310
1	Commandant US Army Command and General Staff College ATTN: Archives Fort Leavenworth, KS 66027
1	Commander US Army Air Defense Human Research Unit ATTN: ATHRD Fort Bliss, TX 79906
1	Chief Concepts Analysis Agency ATTN: CAA-SM 8120 Woodmont Avenue Bethesda, MD 30014
3	Chief of Naval Operations ATTN: OP-05 OP-34 OP-96C2, Mr. Haering Department of the Navy Washington, DC 20305
5	Commander US Naval Air Systems Command ATTN: AIR-604 (3 cys) AIR-530 AIR-09JA Washington, DC 20361
5	Commander US Naval Air Systems Command ATTN: AIR-35603V AIR-330 AIR-5204/PPW, LTC Reimers AIR-5204, CPT W. Rivers AIR-3501, Mr. Fisher Washington, DC 20361
3	Commander US Naval Ordnance Systems Command ATTN: ORD-0632 ORD-035 ORD-5524 Washington, DC 20360

DISTRIBUTION LIST

No. of Copies	Organization
3	Commander US Naval Sea Systems Command ATTN: SEA-6543C, Mr. Sieve SEA-0333, W. W. Blaine SEA-654, CPT J. Frost Washington, DC 20367
1	Chief, Naval Analysis (MCOAG) ATTN: Mr. Jack Watson 1401 Wilson Boulevard Arlington, VA 22209
1	Chief, Naval Materiel Command ATTN: MAT-0315, K. Takle Washington, DC 20360
3	Commander US Naval Air Development Center, Jacksonville ATTN: SR SAED, M. Mitchell SAED, D. Tauras Warminster, PA 18974
2	Commander US Naval Air Propulsion Test Center ATTN: R&T Div, P. Piscopo ATE-4, Mr. Scott Trenton, NJ 08628
1	Commander US Naval Ship Engineering Center Prince Georges Plaza Center Building Hyattsville, MD 21402
1	Commander David W. Taylor Naval Ship Research & Development Center Annapolis, MD 21402
1	Commander US Naval Surface Weapons Center ATTN: Code 040 Silver Spring, MD 20910
4	Commander US Naval Surface Weapons Center ATTN: Code DEC Code GAV, T. McCants W. D. Ralph J. R. Rech Dahlgren, VA 22448
5	Commander US Naval Weapons Center ATTN: Code 408, H. Drake Code 4070, M. Keith Code 4081, C. Sandberg Code 6031, M. Backman Code 4083, G. Monscko China Lake, CA 93555
1	Commander US Naval Ammunition Depot ATTN: RD-3 Crane, IN 47522
1	Director US Naval Research Laboratory ATTN: Code 5554, Dr. Esterowitz Washington, DC 20390
3	Commandant US Marine Corps ATTN: Code AAP AAW-1, LTC Peterson AAW-5, LTC Paige, Jr. Washington, DC 20380
1	Director Development Center, MCDEC Quantico, VA 22134
1	HQ USAF (AFSCAGF) Washington, DC 20330

DISTRIBUTION LIST

No. of Copies	Organization
3	AFSC (LTC Stephenson) Andrews AFB Washington, DC 20331
1	AFSC (SDOA) Andrews AFB Washington, DC 20331
3	HQ USAFSC (XRLW, LTC Seufert; SDW, R. Hartmeyer; DLCA, P. Sandler) Andrews AFB Washington, DC 20334
1	USAFTAWC (OA) Eglin AFB, FL 32542
3	AFATL (DLY) Eglin AFB, FL 32542
1	AFATL (DLRW, W. D. Thomas) Eglln AFB, FL 32542
1	OSU ATTN: Mr. R. Armstrong Eglin AFB, FL 32542
2	AFWL (MAJ H. Rede; MAJ J. Godsey) Kirtland AFB, NM 87117
2	AFSWC (TEEM, LTC D. Meyers; TESPO, MAJ R. Gerhandt) Kirtland AFB, NM 87117
1	TAC (DIO) Langley AFB, VA 23365
4	ASD (ASBR; ASBO, Mr. Erkeneff; ASZT; XOO, Mr. Burneka) Wright-Patterson AFB, OH 45433
3	ASD (ENYS, J. Wallick; J. Howard; L. DiRito) Wright-Patterson AFB, OH 45433
1	ASD (XRHL, G. B. Bennett) Wright-Patterson AFB, OH 45433
4	AFLC (MCNEA, W. Dougherty; PPSC, R. Mergler; MMHM, E. Swanson; MEA, COL T. Egan) Wright-Patterson AFB, OH 45433
4	AFAPL (SFL, Jones; SFH, Botteri; SSF, Churchill; AFH, R. Clodfelter) Wright-Patterson AFB, OH 45433
5	AFFDL (FBS; FER; PTS, D. Voyls; R. Lauzze; CPT Beardon) Wright-Patterson AFB, OH 45433
2	AFML (MAE; MAS, COL Hughes) Wright-Patterson AFB, OH 45433
2	Director National Aeronautics and Space Administration Langley Research Center ATTN: MS 246E, L. Bement MS 249, J. Ward Hampton, VA 23665
1	Director National Aeronautics and Space Administration Lewis Research Center Lewis Directorate Cleveland, OH 44135
1	Bell Helicopter Company ATTN: Mr. Nile Fischer P.O. Box 482 Fort Worth, TX 76101
1	The Boeing Company Vertol Division ATTN: Dave Harding P.O. Box 16858 Philadelphia, PA 19142

DISTRIBUTION LIST

No. of Copies	Organization
1	Fairchild Industries Fairchild Republic Division ATTN: D. Watson Farmingdale, LI, NY 11735
1	Falcon Research and Development Company ATTN: Lavelle Manhood 1225 South Huron Denver, CO 80223
1	Falcon Research and Development Company ATTN: Arthur Stein One American Drive Buffalo, NY 14255
1	General Electric Company Military Engine Products Div ATTN: E. L. Richardson Building 2406A 1000 Western Avenue West Lynn, MA 01910
1	Summa Corporation Hughes Helicopter Division ATTN: J. H. Tinley Centinela and Teale Streets Culver City, CA 90230

No. of Copies	Organization
1	LTV Aerospace Corporation Vought Systems Division ATTN: D. M. Reedy - Unit 2 54244 P.O. Box 5907 Dallas, TX 75222
1	Rockwell International Los Angeles Aircraft Division ATTN: R. L. Moonan Mail Code AB75 International Airport Los Angeles, CA 90009
1	United Aircraft Corporation Sikorsky Aircraft Division ATTN: J. B. Foulk Stratford, CT 06602

Aberdeen Proving Ground

Marine Corps Ln Ofc
Cdr, USATECOM
ATTN: Mr. Moshang
Dir, USAMSAA
ATTN: J. Lindenmuth
D. O'Neill
J. McCarthy